AN ABSTRACT OF THE DISSERTATION OF

Kuo-Fu Tseng for the degree of Doctor of Philosophy in Molecular and Cellular Biology Program presented on December 16, 2013.
Title: Dissecting the Cytoskeletal Interaction during Cytokinesis and the Role of Myosin II Motors on Homologous Chromosomes.

Abstract approved: _____
Dahong Zhang

Prior to cell cleavage, cytokinetic proteins are recruited into the nascent actomyosin contractile ring. Interactions between spindle microtubules and the cell cortex play a critical role in this recruitment. However, direct evidence for physical interaction between microtubules and the cortex has been lacking. Here we reveal the physical connection between astral microtubules and cortical actin filaments, by micromanipulating the fluorescently tagged cytoskeleton in living grasshopper spermatocytes. When microtubules were tugged with a microneedle, they in turn pulled on cortical actin filaments, interrupting the filaments' journey toward the equator. Further displacement of the actin dragged the cell membrane inward, demonstrating that the cortical actin network physically linked spindle microtubules to the cell membrane. Regional disruption of the connection by breaking spindle microtubules prevented actin accumulation in a segment of the ring, which locally inhibited furrowing. Dynamic astral microtubules were shown to be able to move actin aggregates with their tips in Cytochalasin D-treated cells. These data support our model in which dynamic astral microtubules physically redistribute cortical actin into the incipient contractile ring.

During meiosis, homologous chromosomes pair, synapse, and commonly

exchange genetic material, creating genetic variation among offspring. These meiotic specific events take place in prophase I nucleus to ensure the formation of paired homologous chromosomes. However, the source of the mechanical forces that drive chromosome pairing and crossing over remains unclear. Here we show the dynamic distribution of phosphorylated myosin II between the homologous chromosomes during meiosis in grasshopper spermatocytes. The phosphorylated myosin II was localized specifically to paired homologues that undergo crossing over. The myosin II remained phosphorylated during prophase and metaphase, then became abruptly dephosphorylated at anaphase onset, which coincided with separation of the homologues. Pharmacological dephosphorylation of myosin II in prophase dissembled SMC3 axis in pachytene cells and induced partial separation of homologues in diakinesis cells. These results suggest that the activated myosin II motors could provide forces for pairing and/or other meiotic processes of the homologues. Furthermore, inactivation of the motors could be required for dissolution of the chiasmata at the onset of anaphase I, allowing separation of the bivalents. I anticipate that our results will initiate a reassessment of how homologous chromosomes recombine and separate during meiosis, expanding upon the conventional perception of myosin II motors in cell contraction and motility. This basic research could provide a foundation for understanding and eventually treating a subset of medical conditions that arise from meiotic errors.

Dissecting the Cytoskeletal Interaction during Cytokinesis and the Role of Myosin II Motors on Homologous Chromosomes

by

Kuo-Fu Tseng

A DISSERTATION

submitted to

Oregon State University

in partial fulfillment of
the requirements for the
degree of

Doctor of Philosophy

Presented December 16, 2013
Commencement June 2014

Doctor of Philosophy dissertation of Kuo-Fu Tseng presented on December 16, 2013.

APPROVED:

_____

Major Professor, representing Molecular and Cellular Biology Program

_____

Director of the Molecular and Cellular Biology Program

_____

Dean of the Graduate School

I understand that my dissertation will become part of the permanent collection of Oregon State University libraries. My signature below authorizes release of my dissertation to any reader upon request.

_____

Kuo-Fu Tseng, Author

ACKNOWLEDGEMENTS

I would like to express the deepest gratitude to my major professor, Dr. Dahong Zhang. This dissertation would not be possible without his guidance and support. I also thank Dahong for his patience in correcting my writing and presentation skills. I also want to thank my lab mates, Margit Foss and Yunhan Duan, for their help and friendship. In addition, I thank Wei Chen for helping me solve technical problems.

I would like to thank my committee members, John Flower, Jeffery greenwood, Dan Rockey, Arup Indra, for their expertise and time in directing my dissertation. I thank office staff in MCB program and Zoology Department for their kind assistance. I also want to thank Dr. Joe Beatty and Dr. Robert Mason for Teaching Assistantships.

TABLE OF CONTENTS

TABLE OF CONTENTS (Continued)

LIST OF FIGURES

DEDICATION

I dedicate this work to my wife, my son, my daughters and my parents, for their unlimited support.

Dissecting cortical actin movement during cytokinesis and the role of myosin II on meiotic I chromosomes

Chapter 1

Introduction

Accurate chromosome segregation and cytokinesis are essential to maintaining genomic integrity of the offspring. Studies had showed that errors in any of these events will result in abnormal karyotype which could lead to genetic disease or even cancer. For example, the nondisjunction of human chromosome 21, will lead to Down Syndrome (Shen et al., 1998). Tetraploids resulted from cytokinesis failures in mouse oral epithelia cells could promote tumorigenesis (Fujiwara et al., 2005). To prevent or look for a cure of these diseases, it is important to understand the fundamental mechanisms of cell division. My PhD research focused on dissecting the physical interaction between spindle microtubules and cortical actin filaments during cytokinesis and exploring the possible role of phosphorylated myosin II in chromosome pairing and crossing over, and/or chromosome segregation during meiosis I.

1.1 Dissecting the recruitments of cortical actin filaments during cytokinesis

Cytokinesis is the last step of cell division in which a cleavage furrow

forms at the equator to pinch the dividing cell into two daughter cells. Prior to cell cleavage, cytokinetic proteins are recruited into the nascent actomyosin contractile ring at the equatorial region for the assembly of the contractile ring, which contracts to pull the equatorial membrane inward forming cleavage furrow (Rappaport, 1996). This process requires the interaction between spindle apparatus and cell cortex. For example, in sea urchin eggs, furrow initiation requires contacts between astral microtubules and the cortex (Strickland et al., 2005). Disassembling microtubules by Nocodazole changes the cortical distribution of activated myosin II in sea urchin eggs (Foe et al., 2008). Disassembly of microtubule also blocks the translocation of Rho, a cytokinesis regulator, to the equatorial cortex in Hela cells (Kamijo et al., 2005). Although cytokinesis had been studied for decades, it was still not clear about how spindle microtubules direct the movement of cytokinetic proteins toward the region of furrow formation. The first part of my dissertation was to dissect the recruitments of cortical actin filaments into cleavage furrow.

Polar relaxation and equatorial stimulation are the two prominent models explaining how the spindle apparatus affects the cleavage furrow induction (Maddox and Oegema, 2003). Polar relaxation model states that inhibitory signals are sent out from the spindle apparatus toward the polar region to inhibit the contraction of the cell cortex at the polar region. Therefore a contracting cleavage furrow can only form at the equatorial region (Wolpert, 1960; White and Borisy, 1983). On the other hand, equatorial stimulation model states that positive signals are sent out from the spindle apparatus toward the equatorial cortex to facilitate the formation of cleavage furrow at the equatorial region (Maddox and Oegema, 2003).

The signals could be sent through a subset of astral microtubules around the equatorial region (Devore et al., 1989; Salmon, 1989) or from the anti-parallel microtubules of the spindle midzone (Cao and Wang, 1996; Bonaccorsi et al., 1998; Giansanti et al., 2001). Both models suggest the existence of interaction between the spindle apparatus and the cell cortex. Signals, whether positive or negative, are sent through microtubule-dependent transportation (Atilgan et al., 2012). However, classic manipulation experiments done by Rappaport negated that the physical interaction between the spindle and the cell cortex is essential to stimulate the rearrangement of cortical proteins during furrow formation (Rappaport, 1978). In his experiment, furrow induction was not affected in sand dollar eggs when he used a glass needle to disturb the spindle-cortex interaction by rotating the needle around the spindle. However, this experiment could not rule out the reestablishment of interactions between microtubules and actin filaments right behind the needle, since both cytoskeletal elements are highly dynamic. In fact, as Rappaport noted, the furrow failed to form if the speed of needle rotation exceeded one rpm (Rappaport, 1978). However, polarized cells, such as neuroblasts, can use both spindle-induced and apical-basal polarity-induced furrow positioning pathways to recruit cytokinetic proteins (Cabernard et al., 2010).

The work from Chen et al. in silkworm spermatocytes showed that both polar relaxation model and equatorial stimulation model can take place in the same cell and work together to ensure the cleavage furrow formation(Chen et al.,2008). Astral microtubules can promote the accumulation of actin filaments at the equatorial cortex by stimulating the exclusion of cortical actin filaments at the

polar region. At the same time, the anti-parallel microtubules of the central spindle stimulate the accumulation of actin filaments at the microtubule plus ends through de novo assembly. These actin filaments then are delivered to the equatorial cortex through lateral movement of the microtubules towards the cortex. Both models can also work independently to build the actomyosin-based contractile ring at the equatorial region. In the same study, Chen et al. also showed that the spindle microtubules control the rearrangement of cortical actin filaments. In an experiment, they repositioned the spindle apparatus to one side of a cell with a glass needle, which induced microtubule reorganization growing toward the opposite side of the cell. At the same time, cortical actin filaments were moved by the growing microtubules to the opposite side of the spindle (Figure 1.1A). This microtubule-directed movement of cortical actin filaments can also be induced in grasshopper spermatocytes (Figure 1.1B) (Alsop et al., 2009). These experiments clearly showed that spindle microtubules can direct the movement of cortical actin filaments during cytokinesis. These findings prompt us to propose that the growing astral microtubules could physically interact with the cortical actin network and push the pre-existing cortical actin filaments toward the equatorial cortex during cytokinesis (Figure 1.2).

In this dissertation, I focus on dissecting how microtubules direct cortical actin movement into cleavage furrow during cytokinesis. The physical interaction between spindle microtubules and cortical actin filament before and during furrow formation was directly probed by micromanipulation. Direct evidence was obtained to show that spindle microtubules physically connect to the cortical actin filaments

that are moving toward the region of furrow formation. This physical interaction is required for furrow formation and the recruitment of actin filaments in to the incipient cleavage furrow. To track the movement of individual cortical actin filaments, grasshopper spermatocytes were treated with Cytochalasin D to disassemble the long cortical actin filaments into shorter pieces. In Cytochalasin D-treated cells, dynamic astral microtubules were shown to be able to physically move those aggregates of short actin filaments with their plus ends. Without the cortical actin network, the spindle apparatus lost the physical connection with the cell membrane.

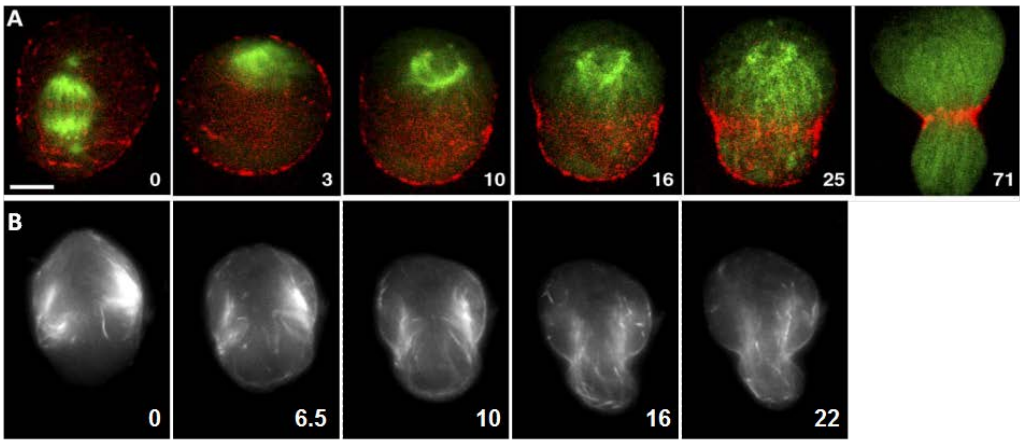

Figure 1.1 Spindle microtubules are able to direct the cortical actin flow
When the spindle apparatus was collapsed and pushed to one side of the cell with a glass needle, cortical actin filaments moved to the other side both in silkworm and grasshopper spermatocytes. A. The silkworm spermatocyte was injected with Alexa-488 tagged tubulin to label microtubules (green) and Rhadomine-phollodin to label actin filaments (Red) Adapted from Chen et al. (2008) B. The grasshopper spermatocyte was injected with Alexa-488 pholloidin to label actin filaments. Adapted from Alsop et al. (2009).

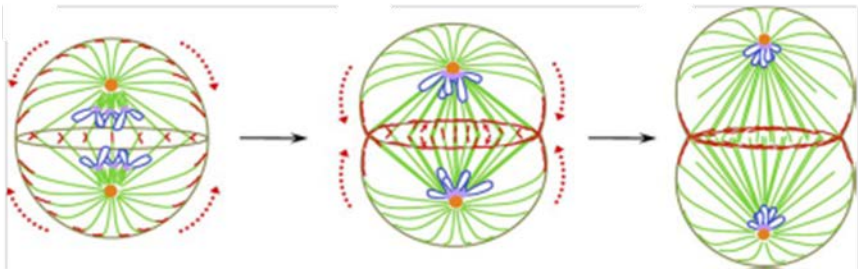

Figure 1.2: Growing astral microtubules physically push pre-existing actin filaments toward equatorial cortex during cytokinesis. Green, microtubules; red, actin filaments; blue, chromosomes; orange, cemtrosomes (Chen et al., 2008).

1.2 The role of myosin II on meiotic I chromosomes

Meiosis is a special cell division for sexual reproduction. Haploid gametes are produced through one round of DNA replication followed by two rounds of cell division, meiosis I and meiosis II. Although meiosis II is similar to mitotic division, meiosis I is specialized for pairing, synapsis, crossing over and separation of homologous chromosomes. Studies have shown that failure of meiotic recombination and segregation of homologous chromosomes in meiosis I would produce gametes with abnormal karyotype (Takaesu et al., 1990; Hassold et al., 1995). Due to the significant role of meiotic recombination in genetics, evolution, and cell biology, meiotic recombination has been studied for over a century. However, it is still unclear about the source of the mechanical forces that pair the homologous chromosomes and cross the chromosome arms during prophase I. The second part of my dissertation is to dissect the possible role of myosin II in the prophase I nucleus and the homologous chromosome segregation.

An overview of meiotic prophase I

The homologous chromosome pairing, synapsis and crossing over take place during prophase I. These meiotic chromosome activities must be completed to ensure the normal segregation during the first meiotic division. Based on the chromosome morphology, prophase I can be divided into 5 stages; leptotene, zygotene, pachytene, diplotene and diakinesis (Wilson, 1928). Duplicated meiotic chromosomes start to seek their homologues and pair with each other in leptotene. In zygotene, the formation of bouquet structure through telomere clustering

promotes homologous chromosome pairing and help the assembly of synaptonemal complex between paired homologous chromosomes. In pachytene, the complete assembly of synaptonemal complex physically connects the homologous chromosome together for the following chromosome crossing over. In diplotene, paired homologous chromosomes desynapse but they are still connected to each other at the spot where crossing over happened. In diakinesis, the nuclear envelope starts to break down. Chromosomes condense and form the typical bivalent chromosome structure (Mckee, 2004). At the DNA level, recombination starts with the appearance of double strand breaks (DSB) in early zygotene. The repairing of these DSBs continues until pachytene, in which synapsis occurs. Some of these DSBs finally lead to crossing over. The arms of paired chromosomes cross over each other to exchange their genetic materials, producing gene recombination during gamete production. The spots of crossing over are called chiasmata, which physically connect the homologous chromosome pair after desynapsis in diplotene (Roeder, 1997).

Homologous chromosome pairing, synapsis and crossing over

Homologous chromosome pairing is the process that meiotic chromosomes look for their homologues and pair with each other. The recognition of homologues is based on sequence similarity (Roeder, 1997; McKee, 2004). In yeast and human, the initial alignment of homologous chromosomes depends on the appearance of meiotic-specific double strand breaks (DSBs). The repairing of these meiosis-induced DSBs and the consequent DNA recombination events

require the interaction with matched DNA on the homologous chromosome. This interaction brings the two homologous chromosomes into alignment. On the other hand, homologous chromosome pairing can also occur in the absence of DSBs in organisms without crossing over like Drosophila and *C. elegans* (MacQueen et al., 2002; Gerton and Hawley, 2005; Ding et al., 2010). Although the mechanism of homologous pairing is still not clear, recent study had suggested that homologous pairing is promoted by the rapid meiotic prophase chromosome movements during leptotene and early zygotene. This rapid chromosome movement increases the chance for meiotic chromosomes to interact with their homologues (Sonntage et al., 2011) as well as tears apart the non-homologous pairings. In fission yeast, the nuclear oscillation-driven telomere-led chromosome movement increases the contacts of homologous chromosomes (Yamamoto and Hiraoka, 2001). The formation of bouquet structure in zygotene also contributes to efficient chromosome pairing (Harper et al., 2004; Lee et al., 2012). The force driving this type of meiotic chromosome movement relies on the existing cytoskeleton outside the nucleus (Koszul et al., 2008; Sato et al., 2009; Fridkin et al., 2009). Nuclear envelope proteins, such as the SUN-KASH protein complex, connect chromosome telomeres to motor proteins outside the nucleus. The sliding of motor protein complex on existing cytoskeleton provides the mechanic force to drive meiotic chromosome movements inside the nucleus. In this way, the mechanic force can be transferred from the cytoplasm into the nucleus to promote telomere clustering and bouquet formation for chromosome pairing. For example, in fission yeast, the SUN is Sad1 and the KASH protein is Kms1. Sad1 is

embedded in the inner nuclear envelope membrane. The N-terminal of Sad1 interacts with the Bqt1 protein complex, which, in turn, interacts with the chromosome telomeres in the nucleoplasm. Kms1 is embedded in the outer nuclear envelop and interacts with dynein motors complex which can move on microtubules. The sliding of dynein on microtubules then drives the chromosome movement inside the nucleus (Chikashige et al., 2007). However, this model cannot explain how the whole strands of these tail-paired chromosomes are brought and held together for the loading of synaptonemal complex. In fact, several studies have suggested that chromosome pairing and synapsis can be done in the absence of bouquet formation, although the efficiency was lower (Lee et al., 2012).

Synapsis takes place with the formation of synaptonemal complex between paired homologous chromosomes. Synaptonemal complex is a tripartite protein structure consisting of two lateral elements (LEs) and one central element (CE)(Yang and Wang, 2009). The lateral elements gradually form along the length on each of the two homologous chromosomes in leptotene. In zygotene, the central element forms right after the two homologues pair with each other to physically link the two lateral elements. In pachytene, the complete loading of synaptonemal complex along the whole length of the homologues indicates the completion of synapsis. Paired homologues are held by synaptonemal complex until the chiasma structure is generated as a result of meiotic crossing over. In diplotene, the central element disassembles but homologues are still held together by chiasma after

desynapsis (Tsai and McKee, 2011). The structure of synaptonemal complex is highly conserved among sexually reproducing eukaryotes (Schmekel et al., 1996). Failures in synapsis will lead to abnormal crossing over and loss of chiasma structure. These meiotic chromosome defects will then affect the spindle assembly in metaphase I. SYCP1, for example, is the protein forming the central element in mice. Most meiotic I cells in SYCP1 knockout mice arrested in pachytene due to the synapsis failure (Kurahashi et al., 2012). MLH1 and MLH3 foci, crossing over markers in late pachytene, were lost when SYCP1 are knocked out in mouse spermatocytes. Meiotic chromosomes formed abnormal chiasma structure in diplotene (de Vries et al, 2005). In C. elegans, knocking out a central element protein, syp-1, leaded to a serve reduction in crossing over (MacQueen et al., 2002). Crossing over failures lead to abnormal bivalent chromosomes and abnormal spindle shape in metaphase I in mouse oocytes (Woods et al., 1999). These findings indicated the importance of synaptonemal complex in holding the homologous chromosomes for DNA recombination. On the other hand, studies also indicated that there could be other mechanisms for the stabilizing of paired homologous chromosomes during prophase I. For instance, the homologous chromosomes still can align and stay together without forming the complete synaptonemal complex in the spermatocytes of SYCP1 knockout mice (de Vries et al., 2005). Analysis of syp-1 mutant of C. elegan also revealed the existence of synapsis-independent mechanism for local stabilizing of homologous pairing (MacQueen et al., 2002).

Myosin II and actin are commonly considered to be the source of force production in a cell since the sliding model was proposed decades ago. However, due to the lack of direct evidence to show the presence of actin or myosin II filaments in the nucleus, it is unclear whether they are able to produce mechanic force in the prophase I nucleus. One possibility is that actin monomers do not form long filaments in the nucleus. These actin filaments could be too short to be detected by phalloidin which was used by researchers to probe actin filaments in the past. On the contrary, antibodies against actin monomer showed the appearance of actin in the nucleus (Gonsior et al., 1999). Recently, several studies showed that actin and myosin II perform critical function without forming filaments in the nucleus. Actin and actin-related proteins (ARPs) have been shown to appear in the nucleus and to be involved in the assembly of the pre-initiation complex and chromatin remodeling (Shumaker et al., 2003; de Lanerolle and Serebryannyy, 2011). The study from Li et al. also showed that myosin II appears in the nucleus of smooth muscle cell and is required for the regulation of ICAM-1 gene expression through interacting with the pre-initiation complex (Li and Sarna, 2009). Myosin II had been shown to localize on chromosome arms in PtK1 cells (Robinson and Snyder, 2005). Myosin II was also localized in prophase I nucleus in crane-fly spermatocytes, although the function of myosin II in prophase I nucleus was not discussed (Silverman-Gavrila and Forer, 2003). It is possible that the mechanic force required for moving chromosomes in the nucleus is much lower than the force for cell mobility or cleavage furrow contraction during cytokinesis. Thus, the

mechanic force generated through the interaction between actin monomer and myosin II on different DNA or nuclear components could be sufficient to move chromosomes without forming filaments (de Lanerolle et al., 2011).

While I was working on the recruitment of myosin II into the cleavage furrow during cytokinesis, I serendipitously found phosphorylated myosin II on metaphase I bivalent chromosomes in grasshopper spermatocytes. This staining pattern of myosin II had never been seen before. In this dissertation, I hypothesized that phosphorylated myosin II could provide the mechanic force to hold the paired homologous chromosomes for pairing, synapsis and crossing over during meiotic prophase I. After anaphase onset, the dephosphorylation of myosin II could be essential for the chromosome separation. The dynamic of myosin II during the meiosis I was determined by immunostaining with an antibody against phosphorylated myosin II. The biological function of myosin II was tested by treating grasshopper spermatocytes with myosin II kinase inhibitors and a myosin II phosphatase inhibitor.

Chapter 2

Astral Microtubules Physically Redistribute Cortical Actin Filaments to the Incipient Contractile Ring

Kuo-Fu Tseng, Margit Foss, and Dahong Zhang

Published in:
Cytoskeleton
350 Main street

Malden MA , 02148
USA
Volume 11, Nov. 2012, 983-991

2.1 Abstract

Prior to cell cleavage, cytokinetic proteins are recruited into the nascent actomyosin contractile ring, paving the way for formation of a functional cleavage furrow. Interactions between spindle microtubules and the cell cortex may play a critical role in this recruitment, since microtubules have been shown to affect distribution and activation of cytokinetic proteins within the cortex. However, direct evidence for physical interaction between microtubules and the cortex has been lacking. Here, we probed the physical connection between astral microtubules and cortical actin filaments, by micromanipulating the fluorescently tagged cytoskeleton in living spermatocytes of the grasshopper *Melanoplus femurrubrum.* When microtubules were tugged with a microneedle, they in turn pulled on cortical actin filaments, interrupting the filaments' journey toward the equator. Further displacement of the actin dragged the cell membrane inward, demonstrating that the cortical actin network physically linked spindle microtubules to the cell membrane. Regional disruption of the connection by breaking spindle microtubules prevented actin accumulation in a segment of the ring, which locally inhibited furrowing. We propose a model in which dynamic astral microtubules physically redistribute cortical actin into the incipient contractile ring.

2.2 Introduction

Over several decades, and with minimal lab equipment, Ray Rappaport developed simple, innovative techniques for mechanically manipulating large egg

cells of marine invertebrates. This allowed him to test hypotheses for cytokinetic mechanisms by physically tweaking or remodeling the potentially dividing cell, and observing how it responded to his various challenges and alterations (e.g., (Rappaport, 1961; Rappaport, 1978)). His pioneering work was an inspiration to scientists who followed him (Pollard, 2004), including ourselves. Among his many classic experiments was a test of the importance of a physical interaction between spindle microtubules and the cell cortex during furrow initiation (Rappaport, 1978). Previous studies had implied that furrow formation was not dependent on this interaction (Hiramoto, 1956; Yatsu, 1912). In Rappaport's experiment, a needle was inserted between the cell membrane and the spindle in a sand dollar egg that was preparing to divide. The tip of the needle was moved repeatedly around the spindle's periphery, inside the egg, with the intention of disrupting any interaction between the cortex and subcortical structures in the cytoplasm such as microtubules. Because the furrow was still able to form, Rappaport concluded that this physical interaction is not essential for furrowing.

In years past, it had been puzzling as to how cytokinetic proteins are recruited into the actomyosin contractile ring during cytokinesis, and the puzzle remains unsolved (Barr and Gruneberg, 2007; Cao and Wang, 1990; D'Avino, 2009; D'Avino et al., 2005; Eggert et al., 2006; Laporte et al., 2010; Noguchi et al., 2001). More recently, evidence has suggested that interactions between spindle microtubules and the cell cortex may indeed play a crucial role in this process. For example, in sea urchin eggs, furrow initiation requires contact between astral microtubules and the cortex (Strickland et al., 2005). This has also been showed in

Drosophila spermatocytes (Glover et al., 2008). In echinoderm zygotes, pharmacological disassembly of microtubules alters the activation pattern of cortical myosin (Foe and von Dassow, 2008). In silkworm spermatocytes, manipulation of dynamic microtubules can drive the flow of cortical actin to the site of cleavage (Chen et al., 2008). Similar flow of cortical actin has also been seen in grasshopper spermatocytes (Alsop et al., 2009) and cultured mammalian cells (Zhou and Wang, 2008). Thus, spindle microtubules can affect distribution and activation of contractile proteins within the cortex, and can influence furrowing. However, a direct physical interaction between spindle microtubules and cortical actin had not been shown.

Our lab has continued in the tradition of physically manipulating relatively large cells to investigate mechanisms of cytokinesis, and Rappaport's work has served as a major catalyst. A key result in this paper, acquired using technology unavailable to Rappaport at the time, has led us to reinterpret some of his earlier data (Rappaport, 1978). Here, we demonstrate a physical connection between astral microtubules and cortical actin, by micromanipulating fluorescently tagged components in living spermatocytes of the grasshopper Melanoplus femurrubrum. We observed that by disrupting the connection, furrow formation could be interrupted. We propose a model in which dynamic astral microtubules contact actin filaments and shepherd them through the cortex toward the incipient actomyosin ring, initiating formation of the cleavage furrow.

2.3 Results and Discussion

We probed, by micromanipulation, for a direct physical interaction between astral microtubules of the spindle apparatus and cortical actin filaments. Dividing, primary spermatocytes from the grasshopper Melanoplus femurrubrum were stained with Oregon Green 488 Taxol and rhodamine phalloidin to visualize the movement of microtubules and actin filaments, respectively. The labeling protocol did not prevent normal progression of cell division, as shown for an unmanipulated control cell (Fig. 2.1A; Movie 2.1 in supplementary material; n = 16 cells; the region of interest in Fig. 2.1A depicts an area in which the interaction would occur in manipulated cells). To test the interaction, a glass microneedle was used to tug the spindle pole – and hence, the astral microtubules – to determine if any actin filaments in the cortex would be dragged by the displaced microtubules. As soon as the astral microtubules were pulled away from the cell cortex, some actin filaments were dragged toward the cell's interior (Fig. 2.1 B-D; Movies 2.2-2.4 in supplementary material), demonstrating a physical link between astral microtubules and cortical actin filaments during cytokinesis. This interaction occurred in mid to late anaphase while actin filaments were recruited into the incipient contractile ring, and later became focused at the contractile ring during telophase. The displaced filaments always followed the direction of aster dislocation, regardless of whether the aster was pulled away from the equatorial cortex (Fig. 2.1B,C; Movies 2.2-2.3; n = 18 cells) or away from the polar cortex (Fig. 2.1D; Movie 2.4; n = 10 cells). Furthermore, the cell membrane

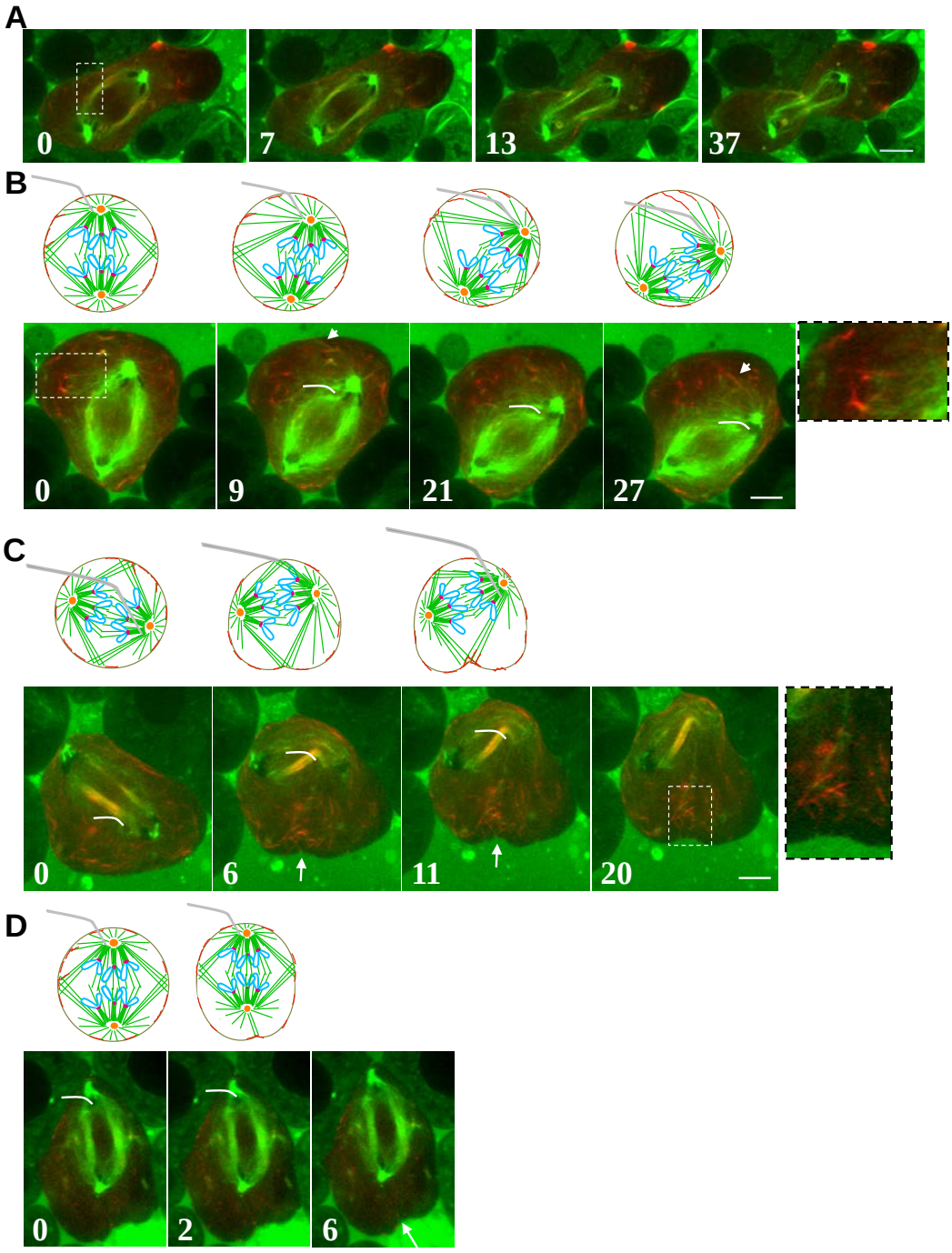
A
0
7
13
37
B
0
9
21
27
C
0
6
11
20
D
0
2
6

Fig. 2.1. Interactions between spindle microtubules and cortical actin filaments were revealed by micromanipulation. (**A**) An unmanipulated dividing grasshopper spermatocyte underwent cytokinesis. Oregon Green 488 Taxol (paclitaxel) diffused into the cell to label microtubules; Texas Red-X phalloidin was microinjected into the cell to label actin filaments. This control cell demonstrated that our labeling protocol neither altered the dynamics of the cytoskeleton, nor impeded the progression of cytokinesis. The region of interest (ROI) highlights the portion of the cell in which interactions between microtubules and actin filaments would have been most clearly visible, had the spindle been manipulated. Time, in min for **A**. (**B**, **C**) As a jointed-glass microneedle (gray bent line in the schematic diagram; superimposed in white on the images) tugged the spindle aster (green) of a living grasshopper spermatocyte towards one side of the equatorial cortex, interconnected cortical actin filaments (red; arrows in **B**) were pulled away from the cortex on the opposite side. The ROI in **B** was enlarged to show the junction between cortical actin filaments and microtubules. Sometimes the membrane was also dragged inward (arrows in **C**). The ROI in **C** shows a network of actin filaments being pulled by a small bundle of microtubules. In the diagrams: spindle microtubules, green; cortical actin filaments, red; centrosomes, orange; chromosomes, blue; kinetochores, magenta; microneedle, gray. (**D**) When one aster was tugged with a microneedle toward its polar region, again actin filaments (red; arrows) were pulled away from the cortex, dragging the membrane inward from the opposite polar region. All cells in Fig. 2.1 were labeled as described in Fig. 2.1A. Panels in **A**-**D** were taken from Movies 2.1-2.4, respectively. Time, in sec for **B**-**D**. Scale bars, 10 μm.

that was adjacent to the displaced filaments could also be pulled inward by further tugging on astral microtubules (Fig. 2.1 C,D; Movies 2.3-2.4) with a microneedle. With sufficient tugging, cortical actin filaments could eventually be broken away from the microtubules and/or from the indented cell membrane, which, relieved of tension, reverted to its original position (Movies 2.3-2.4). The actin filaments that pulled away from the membrane were still connected to the plus-ends of the astral microtubules, resembling fish hooked by a fishing line, while other filaments remained at the cortex. The rapid regression of the membrane after the filaments were pulled away indicated a strong physical connection among microtubules, actin filaments, and the cell cortex. Conversely, the filaments remained in place if the control manipulation was performed without moving spindle microtubules. Since the actin tracked the needle's movement only when microtubules were being dragged, the needle was moving the filaments only indirectly, via the microtubules.

We had previously shown that collapsing a spindle and relocating its asters to one side of the cell by micromanipulation could trigger the flow of cortical actin toward the opposite side. In other words, microtubules from the newly created monopolar spindle elongated toward and interacted with the cortex, resulting in the directionally biased movement of actin away from the spindle pole (Alsop et al., 2009). We had hypothesized that the microtubules contacting the cortex caused the flow, but had not demonstrated a physical link. Here, we directly probed the physical interaction between microtubules and actin filaments during the induced flow of cortical actin, following dislocation of a reorganizing monopolar spindle.

We again observed an interaction (Fig. 2.2A, B; Movie 2.5 in supplementary material; n = 8 cells). The plus ends of some astral microtubules appeared to contact the mobile cortical actin filaments, and the filaments in turn linked the microtubules to the cell membrane (Fig 2.2B). As observed previously (Fig. 2.1C,D), the physical linkage between the three components was so strong that the membrane was dragged significantly inward by the displaced microtubules (Fig. 2.2A; Movie 2.5). When actin filaments were pulled out of the cortex, or detached from the plus ends of microtubules, the cell membrane rapidly relaxed, just as was seen in Movies 2.3 and 2.4. Our experiment demonstrated that the physical connection between microtubules and actin filaments persisted during cortical flow, and was robust enough to withstand movement of either component. Moreover, the connection was not dependent on interdigitating spindle microtubules, which helped substantiate a mechanism by which astral microtubules could affect the distribution of cortical proteins during cytokinesis. We hypothesized that the interaction between spindle microtubules and cortical actin contributes to the formation of the cytokinetic furrow. We tested our idea by blocking this interaction on one side of the cell but not the other. The spindle was confined to one side of the cell by pushing on its lateral face using a microneedle. Spindle microtubules were thus impeded from reaching the region of equatorial cortex distal to the spindle, due to micromanipulation that either brokemicrotubules or detached them from the cortex. As predicted, the cleavage furrow subsequently formed only on the side of the equatorial cortex that the microtubules could readily access (Fig. 2.3A; Movie 2.6 in supplementary material; n = 17 cells). Likewise, movement of

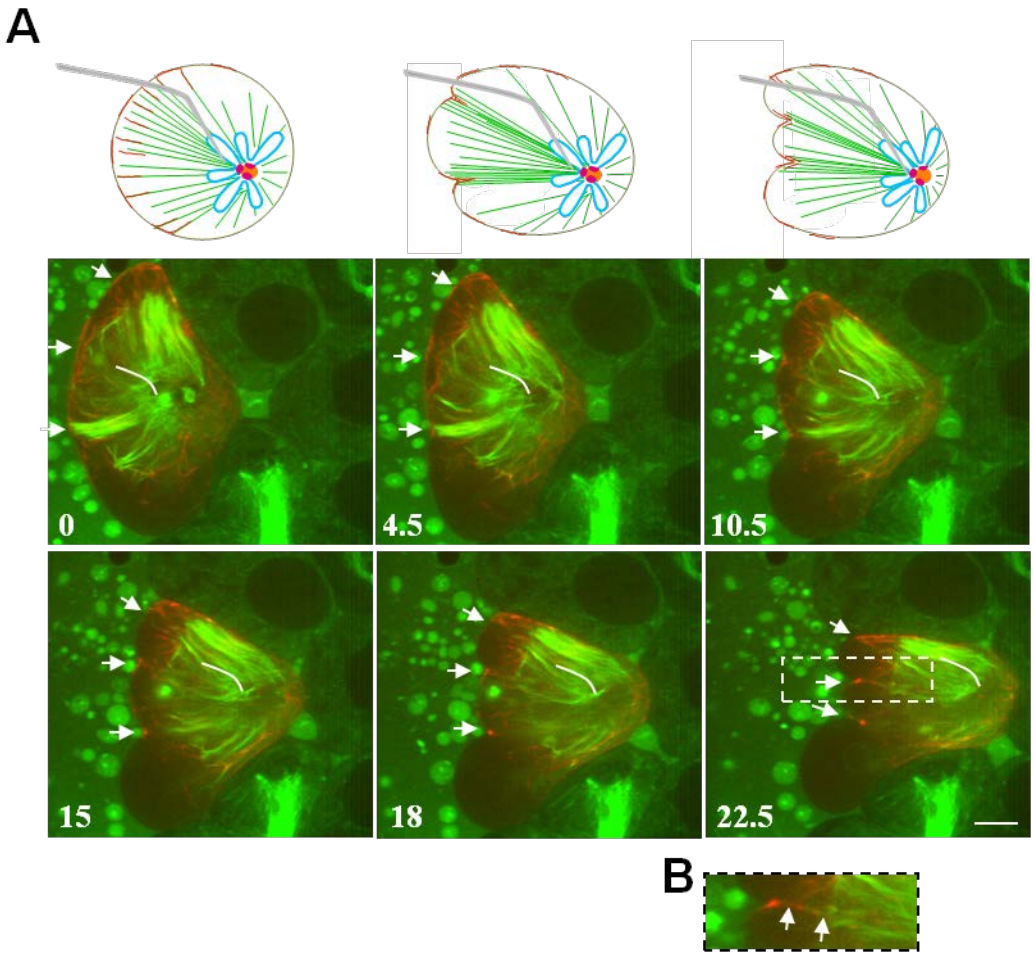

Fig. 2.2. Microtubule interaction with flowing cortical actin filaments, as seen by manipulation of an aster in a monopolar spindle. (**A)** The cortical actin (red) was induced to flow toward the upper and left side of the cell, away from the fused spindle asters (green; near tip of needle in first panel) following manipulation-induced spindle reorganization. As the aster was dragged with a microneedle (bent white line) toward the right side of the cell, cortical actin filaments on the opposite side were displaced along with microtubules. Actin filaments in turn pulled the membrane inward in several places (arrows). Schematic diagrams color-coded as in Fig. 2.1. (**B**) The ROI in **A** was enlarged to highlight a connection between a microtubule (green; arrow on right) and a cortical actin filament (red; arrow on left). Microtubules and actin were labeled as in Fig. 2.1. Panels are from Movie 2.5. Time, in sec. Scale bar, 10 μm.

cortical actin filaments toward the equator was most evident on that same side. Moreover, the distribution of actin filaments confirmed that only a partial contractile ring was able to assemble in such a manipulated cell (Fig. 2.3B; Movie 2.7 in supplementary material).

Species-specific differences could explain the discrepancy between the classic data (Rappaport, 1978) and our data, regarding the necessity of a microtubule/actin interaction for furrowing. Alternatively, there may be a technical explanation. During cytokinesis, microtubules and actin filaments are highly dynamic, as are the interactions between microtubules and the cortex. Thus, the interaction disrupted by the needle in the sand dollar experiment could be rapidly re-established, which would not be readily apparent without fluorescence microscopy. In our experience, the manipulated cells in grasshopper spermatocytes could complete cytokinesis and form an uninterrupted contractile ring, if – midway through the experiment – we stopped disrupting the microtubule-cortex interaction. Indeed, Rappaport noted that furrowing was reduced if his needle exceeded a certain speed. This is consistent with the idea that the interaction in the sand dollar eggs had not been sufficiently disrupted to prevent furrowing. Incidentally, it is likely that earlier experiments, in which cells were seen to furrow in the absence of spindles (Hiramoto, 1956; Yatsu, 1912), were actually revealing the phenomenon of incomplete furrowing, due to contraction of randomly congregating contractile elements.

Our demonstration that spindle microtubules appeared to be physically connected to the flowing cortical actin filaments (Fig. 2.2) suggested that

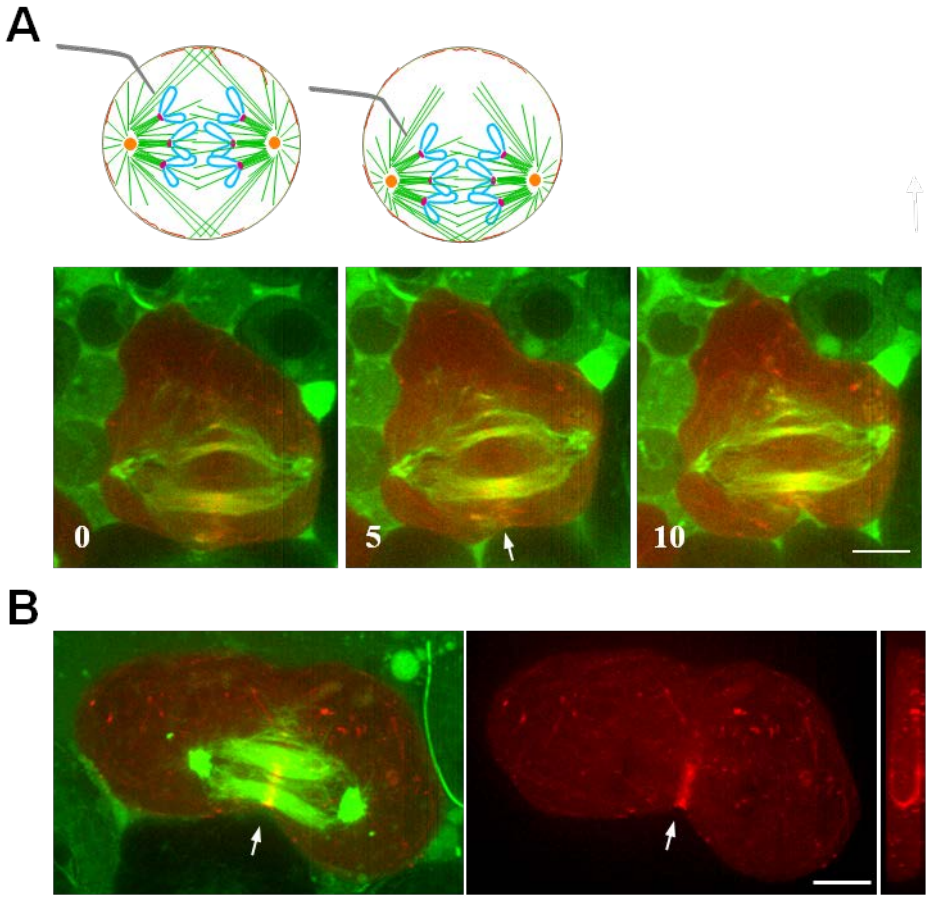

Fig. 2.3. The formation of the cleavage furrow required the physical interaction between spindle microtubules and cell cortex. (**A**) After the spindle was repositioned by pushing on its lateral face with a microneedle, which also broke microtubules, or detached them from the cortex, the cleavage furrow (arrows) formed only on the side proximal to the spindle. Time, in min for Fig. 2.3**A**. Schematic diagrams color-coded as in Fig. 1. Cells were labeled as in Fig. 1. (**B**) A cell that was manipulated as in **A** (before being fixed and stained, as in Materials and Methods) formed only a portion of the contractile ring, as gauged by the distribution of actin. The density of actin was highest in the cortical region closest to the spindle equator, and decreased progressively with increasing distance from the microtubules. Spindle microtubules (green) are shown overlaid with actin (red) from the contractile ring (left panel). Rotation of the stacked images (middle and right panels) revealed the 3D distribution of actin within the malformed contractile ring. The image in the right panel is rotated 90 degrees from that in the middle panel. Panels in **A** and **B** were taken from Movies 2.6-2.7, respectively. Scale bars, 10 μm.

microtubules have the ability to affect the movement of cortical actin filaments in grasshopper spermatocytes. To test if the flow of cortical actin could instead help reorganize microtubules, as proposed for monopolar cytokinesis in HeLa cells (Hu et al., 2008), we disassembled actin filaments by treating the living cells with Cytochalasin D (CD) (Fig. 2.4; Movies 2.8-2.10 in supplementary material). The CD treatment disassembled long actin filaments within the cortex into short segments that coalesced into small, but readily visible aggregates. These CD-disassembled actin aggregates morphologically resembled the de novo-assembled actin aggregates seen in silkworm spermatocytes (Chen et al., 2008), and were comparable to the latrunculin B-induced aggregates from partially disassembled actin in HeLa cells (Hu et al., 2008). We tested both drugs in spermatocytes and chose to use CD for our experiments. Although both treatments achieved the same outcome with respect to actin disassembly, CD had little or no adverse effect on image clarity compared to that of latrunculin B.

As soon as CD-induced actin aggregates became snagged on the plus-ends of astral microtubules, they moved in concert with the elongation and shrinkage of the microtubules before being released. (Fig. 2.4A; Movies 2.8-2.9; n = 11). These attached aggregates could also move laterally or vertically with respect to the imaging plane, due to the waving motion of the microtubules. Therefore, the movement of the aggregates appeared to be synchronized with the dynamics of astral microtubules that were elongating, shrinking, and/or waving (Fig. 2.4A; Movies 2.8-2.9). Occasionally, the spindle happened to be confined asymmetrically in an ultra-flat cell. This made it possible to track

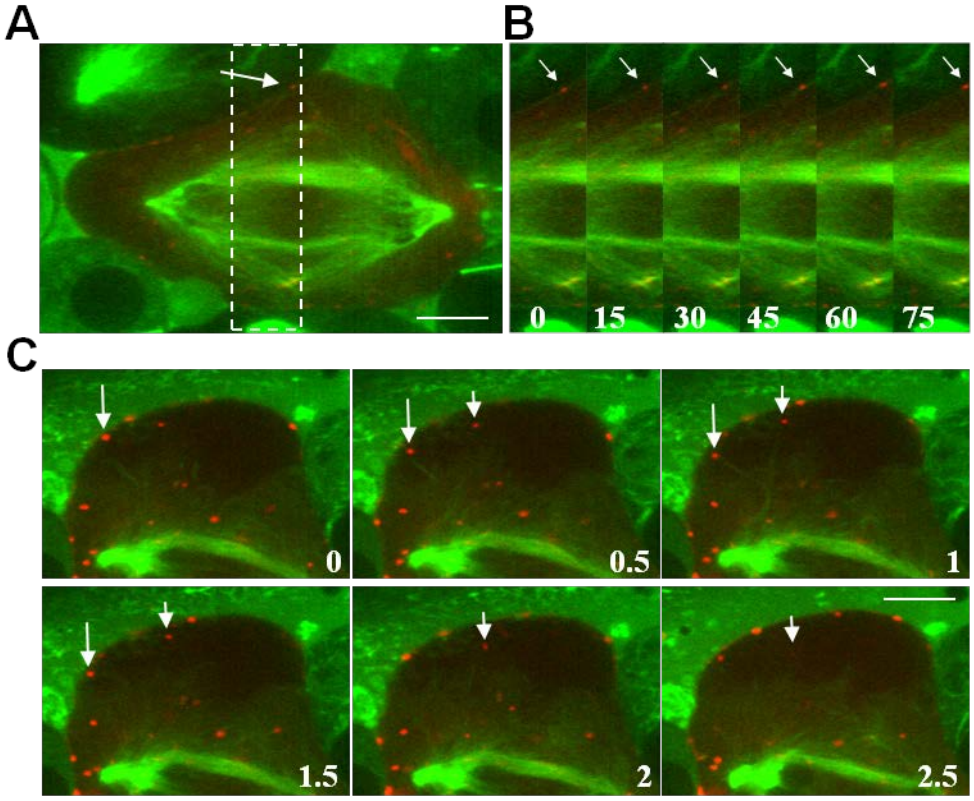

Fig. 2.4. Waving microtubules moved Cytochalasin D-induced cortical actin aggregates. (**A**) Treatment of the spermatocytes with Cytochalasin D resulted in disassembly of some actin filaments and formation of actin aggregates (arrow; actin in red). A few spindle microtubules (green) were seen in the vicinity of aggregates. (**B**) Time-lapse sequence of the ROI in (**A**) revealed the movement of an actin aggregate (arrows) tracking that of a waving microtubule. However, the aggregate did not move consistently in one direction. Time, in sec. (**C**) The spindle happened to be situated toward one side of the cell, creating a region with only a subset of the spindle microtubules growing toward the cortex. The relative sparsity of these microtubules (green) made it easier to observe their interactions (arrows) with actin (red). Time, in min. Cells were labeled as in Fig. 2.1. Panels in **A**, **B** and **C** were from Movies 2.8, 2.9 and 2.10, respectively. Scale bar, 10 μm.

microtubule-aggregate interactions in a less congested environment with better clarity, as the cortical region distal to the spindle had fewer microtubules in a single plane of focus (Fig. 2.4C; Movie 2.10; n = 16 cells).

Notably, the microtubule dynamics appeared unaffected by CD treatment (Movie 2.11 in supplementary material; n = 14; compare to Movie 2.2 or 2.6), as both shortening of kinetochore fibers and poleward chromosome movement progressed normally. Moreover, astral microtubules still elongated and waved in CD-treated cells (Movie 2.11). They could still “pivot” around the centrosomes such that their plus ends swept from pole to equator, interdigitating with microtubules from the opposite pole, just as they would have in untreated cells. If functional cortical actin were required to organize astral microtubules (rather than vice versa), microtubule redistribution to their appropriate destination would have been affected in CD-treated cells. We reasoned that CD’s partial disassembly of cortical actin filaments generated aggregates that could no longer be efficiently swept toward the equatorial cortex by astral microtubules, even though the behavior of the microtubules seemed otherwise unperturbed. Under these conditions, formation of the cleavage furrow was blocked. Our findings support the idea that dynamic microtubules can physically move cortical actin filaments into the incipient contractile ring to advance furrow formation. These data are also consistent with our observations that, in silkworm spermatocytes, cortical flow of untreated actin is dependent on dynamic microtubules as it can be disrupted by treatment with taxol (Chen et al., 2008).

We noted differences in the behaviors of CD-induced actin aggregates and

untreated cortical actin filaments. First, tugging on astral microtubules in non-CD-treated cells pulled the cell membrane inward, and eventually dislodged cortical actin filaments. In contrast, after the actin network was impaired by CD treatment, tugging these microtubules with a microneedle no longer caused membrane ingression (Fig. 2.5; Movie 2.12 in supplementary material; n = 10 cells). Second, the aggregates appeared to have less directionality than the filaments that were not disassembled, and did not progress steadily toward the equator (Fig. 2.4; Movies 2.8-2.9). These differences suggested that the cortical actin network physically links spindle microtubules to the cell membrane (Fig. 2.1C,D). The linkage between spindle microtubules, cortical actin, and the cortex was apparently weakened by filament disassembly and aggregation, indicating that the CD treatment may have undermined interactions with proteins that bind filamentous actin (e.g., ERMs at the plasma membrane (Carreno et al., 2008; Fehon et al., 2010; Kunda et al., 2008)). As expected, the spindle could be moved around more easily, i.e, with less resistance, by a microneedle within the CD-treated cell than in an untreated cell (Fig. 2.5; Movie 2.12). These findings suggested that the interaction between the actin filaments and the cell membrane helps provide the directionality for the microtubule-driven cortical flow of actin towards the incipient contractile ring.

Based on our data in grasshopper spermatocytes, we propose a model in which dynamic astral microtubules physically move or sweep the preexisting cortical actin filaments toward the incipient contractile ring during cytokinesis, thus contributing to the ring’s assembly. Elongation of microtubules could provide

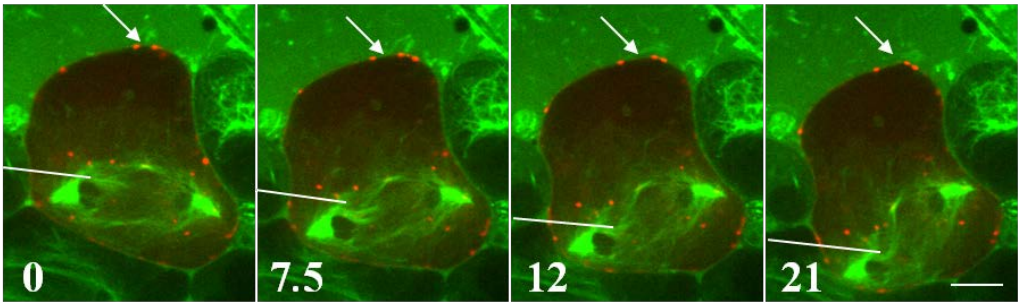

Fig. 2.5. The connection between membrane and microtubule was mediated by the actin network. In the presence of Cytochalasin D, the membrane could no longer be pulled inward by spindle microtubules (green) that were displaced using a microneedle (shown as straight line), as compared to the untreated cells shown in Figs. 2.1 and 2.2. No membrane indentation was discernible at the upper side of the cell (arrow) when the spindle was pushed downward, despite the presence of actin aggregates (red). Cells were labeled as in Fig. 2.1. Panels are from Movie 2.12. Time, in sec. Scale bar, 10 μm.

the driving force. Perhaps, a microtubule tip-binding protein such as EB1, which also interacts with actin filaments (Akhmanova and Steinmetz, 2008; Basu and Chang, 2007; Galjart, 2010), could mediate the interaction between microtubule plus ends and cortical actin filaments. EB1 has been shown to localize to astral microtubules (e.g., (Rankin and Wordeman, 2010) in HeLa cells). Actin filaments may be moved to the vicinity of the equatorial cortex or directly to the incipient ring (Alsop et al., 2009). This relocalization will increase their chances of interacting with other proteins involved in ring formation, such as myosin II (Foe et al., 2000; Noguchi et al., 2001); septins (Estey et al., 2011; Joo et al., 2007), RhoA (Bement et al., 2005; Piekny et al., 2005), or the scaffolding protein anillin (D'Avino et al., 2008; Field and Alberts, 1995; Goldbach et al., 2010; Piekny and Maddox, 2010). Some of these proteins have been shown to interact with microtubules and/or cortical actin (e.g., (Foe et al., 2000; Sisson et al., 2000)). We envision the cortical actin filaments being tethered to actin binding proteins throughout the cortex. The progressive movement of actin towards the equatorial cortex requires frequent bouts of dissociation, during which astral microtubules can bind the filaments (perhaps via EB1), and sweep them closer to the equator before they become re-anchored to the cortex. This ratcheting effect would ensure a unidirectional flow of actin toward the equator.

Actin throughout the cell is likely transported to the incipient contractile ring by more than one mechanism, in addition to cortical flow (Alsop et al., 2009; Chen et al., 2008). For example, we had shown in silkworm spermatocytes that de novo actin assembly could take place at the plus ends of bundled central spindle

microtubules (Chen et al., 2008), and had seen actin in the same location in grasshopper spermatocytes (Alsop et al., 2009). These de novo assembled actin filaments are transported laterally via the splaying of central spindle microtubules toward the equatorial cortex, thus aiding formation of the ring (Chen et al., 2008). Likewise, vesicle-associated actin (Albertson et al., 2008) may also undergo lateral transport to the furrow (Chen et al., 2008) by the array of microtubule bundles at the base of ingressing furrows (Larkin and Danilchik, 1999; Larkin and Danilchik, 2001). Furthermore, preexisting cytoplasmic actin filaments could also contribute to ring formation, potentially through their transport on spindle microtubules (Alsop et al., 2009). We note the distinction between dynamic and stable astral microtubules, as have others, e.g., (Foe and von Dassow, 2008; Odell and Foe, 2008). In grasshopper spermatocytes, astral microtubules are highly dynamic in anaphase, which is essential to driving cortical flow. As anaphase progresses, most astral microtubules from opposite poles become trapped and stabilized as their plus ends interdigitate adjacent to the equatorial cortex (Fig. 2.4A). We think that the interdigitating microtubules at the furrow region are derived from both the astral microtubules that have swept cortical actin to the equator, and the central spindle microtubules that have engaged in lateral transport of de novo assembled actin filaments. These two classes of microtubules, both before and after interdigitating at the cortex, could provide tracks along which cytoplasmic actin filaments could be delivered to the equator (Alsop et al., 2009). Moreover, the interdigitating microtubules could conceivably provide a stable bridge for transport of structural or regulatory proteins to the equatorial cortex – perhaps in preparation for furrow

ingression and abscission (Guizetti and Gerlich, 2010).

2.4 Materials and Methods

Primary Cell Culture

Primary spermatocytes of the grasshopper Melanoplus femurrubrum were prepared as previously described (Alsop and Zhang, 2003). Briefly, the cells were spread in a monolayer onto a coverslip under Halocarbon oil (Halocarbon 400). During spreading, spermatocytes were flattened under the oil. Naturally, some cells were spread flatter than others, allowing us to obtain higher image clarity by taking advantage of these inevitable variations.

Staining of Microtubules and Actin Filaments in Living Cells

Microtubules were labeled by micropipetting Oregon Green 488 Taxol (Tubulin Tracker Green; Invitrogen), diluted to 0.1 mM in insect Ringer's buffer, in the vicinity of the target cells. While pipetting, Tubulin Tracker was (Alsop and Zhang, 2003) further diluted at least 1000 fold by the solution around the target cells. After approximately 5 min, uptake of Tubulin Tracker by the cells was sufficient for visualization and manipulation of the microtubules. By performing the experiments immediately after labeling, exposure of the cells to Taxol was limited to ~20 min or less. Actin filaments were labeled by microinjecting Texas Red-X phalloidin (Molecular Probes/Invitrogen) at 200 units/ml into the target

cells. The microinjection needle was made using a Flaming/Brown P-87 micropipette puller (Sutter Instrument Company) as described (Chen et al., 2008). Control experiments demonstrated that these labeling treatments did not appear to alter the dynamics of the labeled cytoskeleton, nor did they impede the progression of cytokinesis (Fig. 2.1A; Movie 2.1 in supplementary material; n = 16).

Microscopy

Spermatocytes were visualized with an inverted Zeiss Axiovert 135 microscope equipped for spinning disc confocal microscopy (CARV, Carl Zeiss). The microscope is equipped with a 1.4 NA achromatic-aplanatic condenser and a 1.45 NA/100X a-Plan objective (Carl Zeiss). An EM-CCD digital camera (Hamamatsu C9100–12). Images were recorded and processed using Simple PCI software (C-image), and Photoshop software (Adobe Systems) (Alsop and Zhang, 2003). Movies were recorded at one frame every 15 to 30 seconds, except when imaging manipulations, during which the frame rate was increased to approximately one every two seconds.

Micromanipulation

The glass needle for micromanipulation was made using a microforge (Narishige, model MF-830) as described (Zhang and Nicklas, 1999). The needle was controlled by a micromanipulator (Burleigh MIS-5000 series piezoelectric micromanipulator) (Alsop and Zhang, 2003). The extensible cell surface of the grasshopper spermatocyte readily allowed external manipulation of spindle

components. Thus, the microneedle never pierced the cell membrane.

Cytochalasin D treatment

A 5 mg/ml stock solution of Cytochalasin D in DMSO (Sigma-Aldrich) was diluted to 250 g/ml in insect Ringer's buffer. Micro-application of the diluted CD (together with Tubulin tracker green) in the solution surrounding the target cells resulted in a further dilution of greater than 1000 fold. CD-treated cells were immediately injected with phalloidin to label actin filaments. Micromanipulation was performed approximately 3-4 minutes following application of CD, after actin aggregates had formed.

Immunofluorescence Staining

The dividing grasshopper cells, spread on a coverslip, were fixed and stained as described previously (Alsop and Zhang, 2004), with minor modifications. Briefly, cells were first microfixed with 2% glutaraldehyde and 2% paraformaldehyde in PBS, then macrofixed in 0.1% glutaraldehyde and 4% paraformaldehyde in PBS. Microtubules were stained with a 1:100 dilution of Mouse anti-b-tubulin primary antibody (Millipore), and a 1:300 dilution of Goat anti-Mouse Alexa 488 (Molecular Probes/Invitrogen). Actin filaments were stained with 0.165 μM Texas Red phalloidin (Molecular Probes/Invitrogen). Cells were mounted in Vectashield mounting medium (Vector Laboratories).

Chapter 3

Phosphorylated myosin II on homologous chromosomes and its potential role in meiosis I

Kuo-Fu Tseng, Margit Foss, Yunhan Duan & Dahong Zhang

In preparation for submission:
Nature Cell Biology
75 Varick Street, 9th Floor
New York NY 10013-1917
USA

3.1 Summary

During meiosis, homologous chromosomes pair, synapse, and commonly exchange genetic material (Gerton and Hawley, 2005; Ding et al, 2010; Bhalla and Dernburg, 2008), creating genetic variation among offspring. In many eukaryotes, the molecular basis for homologous recombination involves Spo11-catalyzed double-strand breakage within one homologue, and subsequent repair via strand invasion into the partner homologue – resulting in crossing over between nonsister chromatids (Bhalla and Dernburg, 2008). However, the source of the mechanical forces that drive chromosome pairing and crossing over remains enigmatic. Here we show the dynamic distribution of phosphorylated (i.e., activated) myosin II between the homologous chromosomes during meiosis in grasshopper spermatocytes. The distribution of the punctuate phosphorylated myosin II was reminiscent of that of grasshopper chiasmata (Santos et al., 1986; Viera et al., 2004) and the myosin was localized specifically to paired homologues that undergo crossing over. The myosin II remained phosphorylated during prophase and metaphase, then became abruptly dephosphorylated at anaphase onset, which coincided tightly with separation of the homologues. Pharmacological dephosphorylation of myosin II in prophase caused the disassembly of SMC3 axis between homologues in pachytene cells and induced partial separation of homologues in diakinesis cells. Blocking the dephosphorylation of myosin II after anaphase onset prevented chromosomes from separating. Our results suggest that the activated myosin II motors could provide forces for pairing and/or other meiotic processes of the homologues. Furthermore, inactivation of the motors

could be required for dissolution of the chiasmata, i.e., the “chiasmata binder” (Nasmyth, 2001) at the onset of anaphase I, allowing separation of the bivalents. We anticipate that our results will initiate a reassessment of how homologous chromosomes recombine and separate during meiosis, expanding upon the conventional perception of myosin II motors in cell contraction and motility. This basic research could provide a foundation for understanding and eventually treating a subset of medical conditions that arise from meiotic error (Hassold and Hunt, 2001; Kurahashi et al., 2012; Homolka et al., 2012). For example, meiotic sex chromosome inactivation (MSCI) (Burgoyne et al., 2009; Turner, 2007) can be thwarted by the presence of inappropriately unsynapsed autosomes, resulting in infertility (Homolka et al., 2012; Kurahashi et al., 2012; Burgoyne et al, 2009).

3.2 Results and Discussion

While investigating the assembly of the contractile ring during cytokinesis, we serendipitously discovered phosphorylated myosin II on paired homologues during meiosis I in spermatocytes of the grasshopper *Melanoplus femurrubrum*. Using an antibody developed for phosphorylated regulatory light chains of myosin II (pRLC) in mouse (rabbit anti-phospho-Myosin Light Chain 2 (Thr18/Ser19) antibody; Cell Signaling Technology), we revealed spatial and temporal distributions of the activated myosin II from prophase through telophase during the first meiotic division in grasshopper spermatocytes. Phosphorylated myosin II on chromosomes was first detected during the late zygotene stage of prophase I when pairing and synapsis of the homologues take place (Fig. 3.1A). Phosporylated

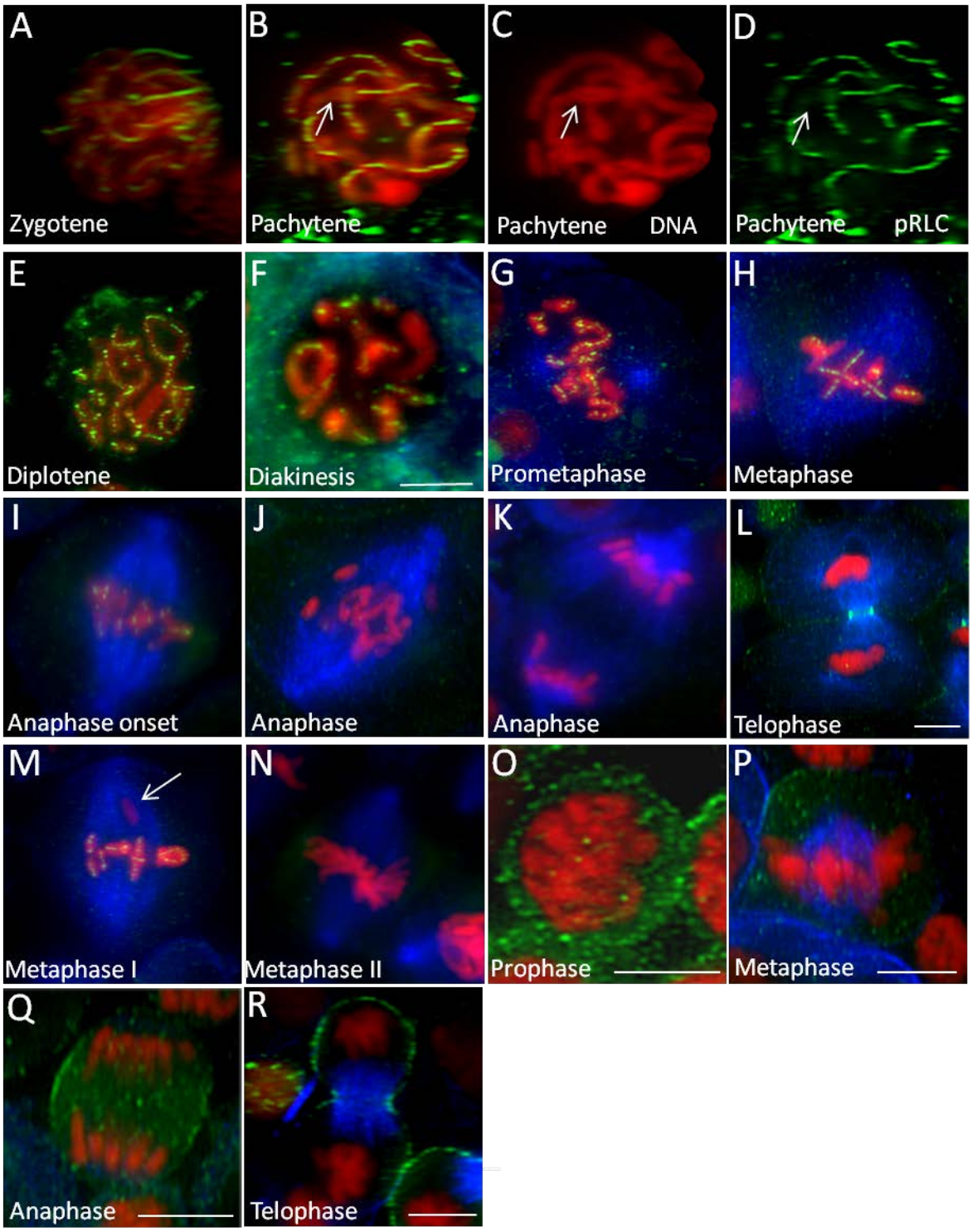
A
Zygotene
B
Pachytene
C
Pachytene DNA
D
Pachytene pRLC
E
Diplotene
F
Diakinesis
G
Prometaphase
H
Metaphase
I
Anaphase onset
J
Anaphase
K
Anaphase
L
Telophase
M
Metaphase I
N
Metaphase II
O
Prophase
P
Metaphase
Q
Anaphase
R
Telophase

Figure 3.1: Dynamic distribution of phosphorylated myosin II during the first meiotic division in grasshopper spermatocytes. Phosphoryated myosin II appeared on synapased homologous chromosomes in prophase I nuclei. It was neither detected on the univalent sex chromosome in meiosis I, or between sister chromatids in meiosis II and on mitotic chromosomes in grasshopper spermatogonia.

A-L, Representative images of various stages through meiosis I. **B-D,** Phosphorylated myosin II was not detected on an unsynapsed homologous chromosome (arrow). **M**, Phosphorylated myosin II was also not detected on the univalent sex chromosome (arrow); **N**, Sister chromatids in meiosis II; **O-R**, Chromosomes during mitosis in grasshopper spermatogonia. (*n>10 cells for each stage in **A-R.***). Green, phosphorylated myosin II; red, chromosomes; blue, microtubules. Scale bar, 10 μm.

myosin II appeared only on synapsed homologous chromosomes (Fig 3.1B-D), but not on an unsynapsed one (Fig 3.1B-D, arrow). The staining intensified during pachytene when crossing over occurs and chiasmata assemble, and became clearly visible along the "suture lines" between the homologues during diplotene (Fig. 3.1E) and diakinesis (Fig. 3.1F) when the fully assembled chiasmata are readily identifiable. The myosin II remained phosphorylated through spindle assembly (Fig. 3.1G) and metaphase (Fig. 3.1H), but began to dephosphorylate at the onset of anaphase (Fig. 3.1I). No phosphorylated myosin II was detected during anaphase (Fig. 3.1J and K), either on chromosomes or in the cytoplasm. Re-phosphorylation of myosin II did not occur until cytokinesis, during which phosphorylated myosin II became concentrated in the contractile ring (Fig. 3.1L).

Notably, phosphorylated myosin II was localized only at the interface between homologous chromosomes in meiosis I. It was seen neither on the univalent sex chromosome in meiosis I (Fig. 3.1M, arrow), nor between the sister chromatids in meiosis II (Fig. 3.1N). Consistent with this result, phosphorylated myosin II did not localize to mitotic chromosomes in grasshopper spermatogonia (Fig. 3.1O-R). Interestingly, phosphorylated myosin II did not localize to meiotic bivalents in drosophila spermatocytes (not shown), which do not undergo homologous recombination. Failure of recognition by the pRLC antibody was highly unlikely, as the antibody stained phosphorylated myosin II elsewhere in these cells. Incidentally, grasshoppers appear to exhibit a meiotic pairing pathway similar to those found in mouse and budding yeast, but absent in other insects, including Drosophila (Vazquez et al., 2002).

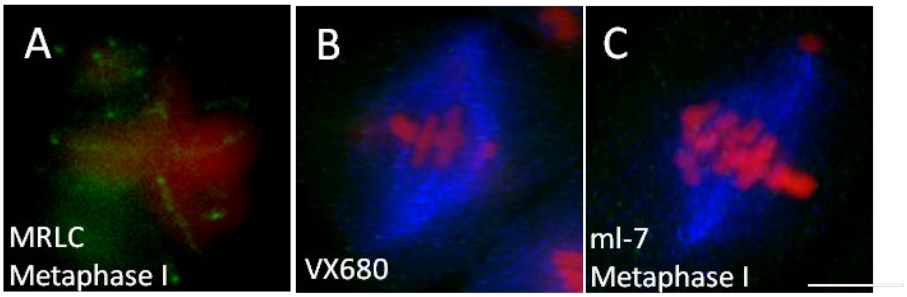

Figure 3.2: Phosphorylated myosin II was not detected on the bivalent chromosomes in spermatocytes treated with kinase inhibitors.

A, Metaphase I bivalents was stained with an antibody against non-phosphorylated myosin II. Green, non-phosphorylated myosin II; red, chromosomes. **B and C**, Metaphase I cells were treated with Aurora B kinase inhibitor VX680(B) or myosin light kinase inhibitor ml-7(C). Green, phosphorylated myosin II; red, chromosomes; blue, microtubules. (*n >10 cells*) Scale bar, 10 μm.

We tested whether our unprecedented observations reflected true distribution patterns and dynamics of myosin II motor proteins, or merely cross-labelling of a phosphorylated epitope on other proteins by the pRLC antibody in grasshopper spermatocytes. Another myosin antibody against non-phosphorylated myosin II light chain (MRLC antibody, Cell Signalling Tech) showed similar staining on metaphase I bivalent chromosomes. (Fig. 3.2 A) The phosphorylation of myosin II on homologous chromosomes could be pharmacologically modulated using various commercially available myosin II kinase inhibitors. For instance, myosin II on the bivalents was completely dephosphorylated by two kinase inhibitors, VX680 (Aurora-B kinase inhibitor that leads to dephosphorylation of myosin II) (Fig. 3.2B) and ml-7 (myosin light chain kinase inhibitor) (Fig. 3.2C). Although the validity of this test rests on the specificity of the inhibitors, it is unlikely that both inhibitors produced false positive results given their demonstrable specificity.

To test if phosphorylated myosin II is involved in homologous chromosome pairing, synapsis and crossing over, prophase I grasshopper spermatocytes were treated with ml-7 to dephosphorylate myosin II. Treated cells were fixed and stained for SMC3 (structural maintenance of chromosome 3) to see the progression of synapsis (Valdeolmillos et al., 2007). In control pachytene cells, the SMC3 axis was a continuous thread along the length of paired homologous chromosomes (Figure 3.3 A-C). However, the SMC3 axis became discontinuous patches along the length of paired homologous chromosomes in ml-7 treated pachytene cells (Fig 3.3 D-E). SMC3 was shown to be required the formation of synaptonemal complex and DNA

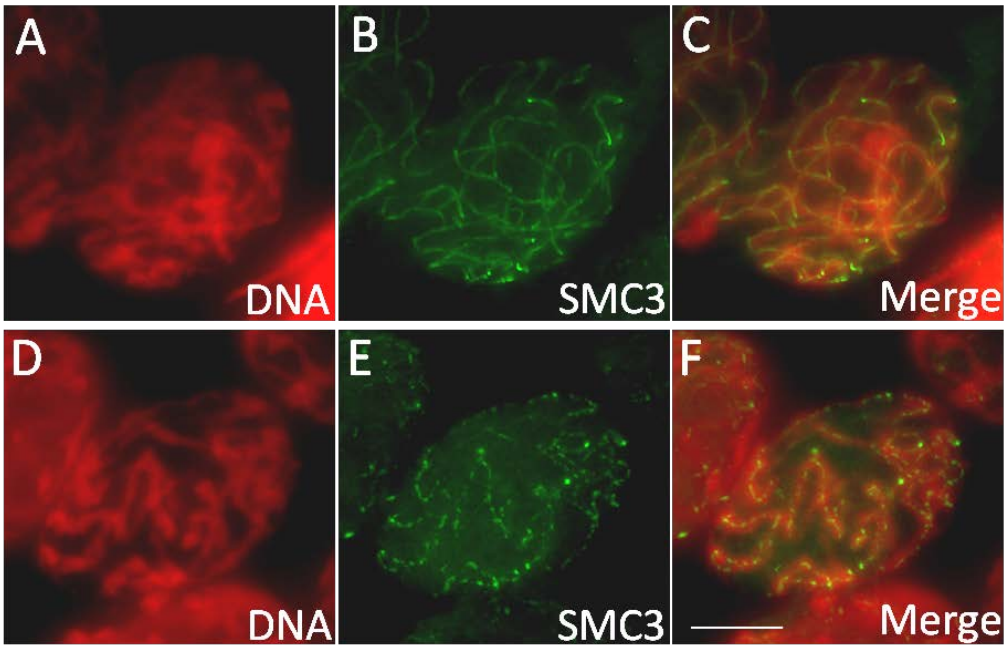

Figure 3.3 Ml-7 caused the disassembly of SMC3 axis between homologous chromosomes in pachytene cells. Comparing to the control in which the SMC3 axis was continuous along the length of homologous chromosomes (A-C), the SMC3 axis in a ml-7-treated cell became discontinuous patches along the length of the chromosomes (D-F). Both the control and the treated cells were in pachytene stage. Red, DNA. Green, SMC3. Scale bar, 10 μm

recombination during meiosis, as well as for sister chromatin cohesion in yeast (Klein et al, 1999). In grasshopper *Paratettix meridionalis*, the maturation of SMC3 axes in pachytene cells was also shown to drive the latter loading of recombinases and therefore determine the chiasma locations in all autosomes (Viera et al., 2009). Here, we show that the dephosphorylation of myosin II caused the disassembly of SMC3 axis between homologous chromosomes in ml-7 treated pachytene cells. This defect could potentially lead to the failures of synaptonemal complex assembly and homologous crossing over.

Precocious dephosphorylation of myosin II on bivalents, induced by ml-7 treatment during diakinesis, also interfered with the maintenance of bivalent structure and condensation of homologous chromosomes (Fig. 3.4). The paired homologues became partially separated along their arms (arrows in Fig. 3.4A depict gaps between partners), and were much less condensed as seen by phase contrast microscopy, compared to bivalents in a control cell at a similar stage (Fig. 3.4B).

Treating metaphase I cells with ml-7 caused misalignment of chromosomes (Movie 3.1). This phenomenon suggested that phosphorylated myosin II could also be involved in the controlling of anaphase onset through affecting the alignment of chromosomes at equator plate. To test this idea, we detached a chromosome from the spindle with a microneedle in the presence of ml-7 and tested if the detached chromosome could move back to metaphase plate. As expected, the detached chromosome could not move back to the equator in the presence of ml-7 (Movie 3.2), whereas in the control cell, the detached chromosome moved back to the

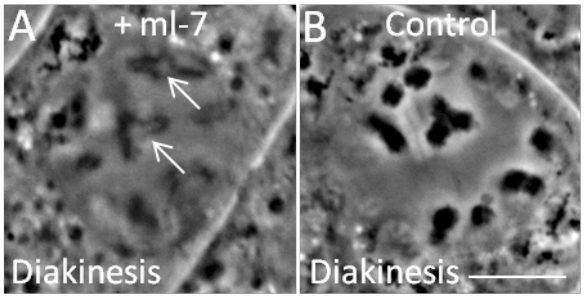

Figure 3.4 Dephosphorylation of myosin II using kinase inhibitor ml-7 induced partial separation and decondensation of homologous chromosomes.

A, Partial separation and decondensation of ml-7-treated chromosomes (arrows show gaps between homologues). **B**, An untreated cell at a similar stage. (*n >10 cells for both **A** and **B***.). Phase contrast microscopy. Green, phosphorylated myosin II; red, chromosomes; blue, microtubules. Scale bar, 10 μm.

equator rapidly (Movie 3.3). Similar results had been shown in crane-fly (Silverman-Gavrila and Forer, 2001). They found that treating prometaphase cells with ml-7 prevented chromosome attachment to spindle in crane-fly spermatocytes. Taken together, these data supported the idea that phosphorylated myosin II could be involved in the controlling of anaphase onset by affecting the chromosome alignment during metaphase I, perhaps through interacting with actin filaments in the spindle apparatus (Fabian and Forer, 2007).

Since phosphorylated myosin II on bivalents rapidly dephosphorylated after anaphase onset, we hypothesized that the dephosphorylation of myosin II could be essential for the separation of bivalents after anaphase onset. If so, blocking myosin II dephosphorylation could prevent the separation of bivalents after anaphase onset. We tested this idea by treating metaphase I cells with calyculin A, a myosin II phosphastase inhibitor, to block myosin II dephosphorylation. The results showed that chromosome separation never happened in the presence of calyculin A. Similar results had been shown in crane-fly spermatocyte (Fabian and Forer, 2007). However, we could not be certain if anaphase onset indeed happened. To solve this problem, we temporally isolated several bivalent chromosomes in a membrane pocket compressed out of a metaphase I cell with a microneedle (Fig. 3.5 A-E). The membrane pocket remained connected to the mother cell via a fine plasma membrane tube, which permitted the isolated bivalents to return anytime into the mother cell by simply decompressing the cell. Therefore, the separation of chromosomes in the mother cell could be used to indicate the time of anaphase

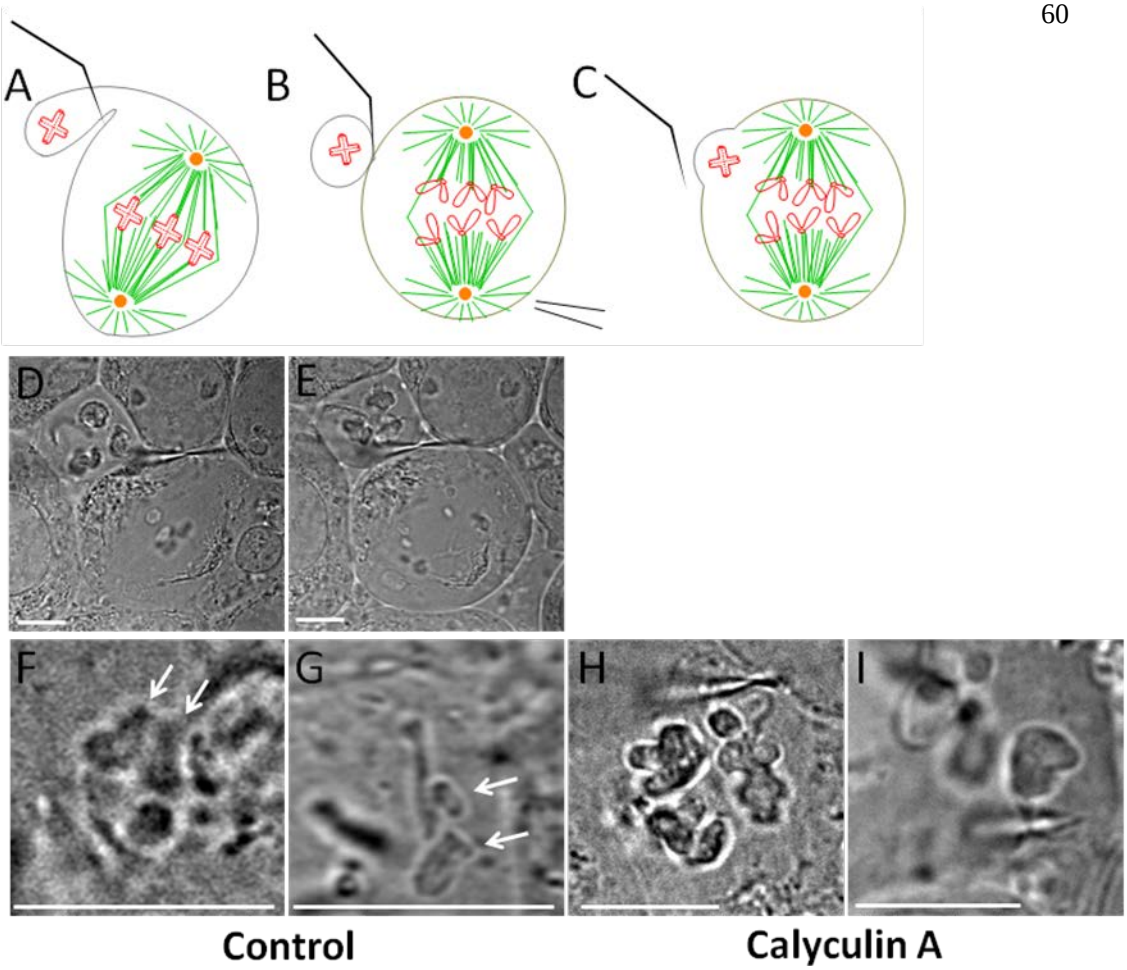

Figure 3.5 Myosin II dephopshorylation is essential for the separation of bivalent chromosomes after anaphase onset.
Several bivalent chromosomes were moved to the edge of a cell and isolated in a membrane pocket by compressing the plasma membrane of mother cell with microneedle (A and D). The microneedle was held between the membrane pocket and the mother cell to keep them apart but remain connected from each other by a fine plasma membrane tube. When the microneedle was removed, the membrane pocket could fuse back to the mother cell and release the isolated bivalent chromosomes back into the mother cell. Calyculin A was pipetted around the manipulated cell to prevent the myosin II dephosphorylation after the anaphase of mother cell started (B and E). Then the microneedle was removed to release the isolated chromosomes back into the anaphase mother cell (C). In control, the temporally isolated bivalent chromosomes completely separated soon after moving back into the anaphase mother cell. The separation of isolated bivalent chromosomes was confirmed by tagging the chromosomes with a microneedle (F and G). In the presence of Calyculin A, the isolated bivalent chromosomes failed to separate after moving back into the anaphase mother cell (H and I). n = 6. Scale bar, 10 μm

onset. Because of isolation, the anaphase onset of the mother cell did not initiate the separation of isolated bivalent chromosomes in the membrane pocket. When the microneedle was removed, the isolated bivalents moved back into the mother cell in anaphase and completely separated (Fig. 3.5 F and G). However, the isolated bivalent chromosomes failed to separate in the anaphase mother cell in the presence of Calyculin A micropipetted around the cell (Fig. 3.5 B) after the anaphase onset took place (Fig. 3.5 H and I). This result indicated that the complete separation of bivalent chromosomes after anaphase onset required the dephosphorylation of myosin II on bivalents.

Previous studies had shown that the increasing of tension on chromosomes before anaphase onset triggered the dephosphorylation of certain tension-sensitive proteins, such as Mad2 and 3F3 antigens (Li and Nicklas, 1995, Nicklas, 1997). To test if the dephosphorylation of myosin II is also triggered by the increasing of tension before anaphase onset, we increased the tension on a bivalent chromosome by pulling the chromosome with a microneedle (Fig. 3.6A and B) or decreased the tension by detaching the chromosome from the spindle (Fig. 3.6C). The manipulated cells were fixed for immunostaining of phosphorylated myosin II after 10 minutes of pulling or detaching. The results of staining showed that the amount of myosin II phosphorylation on the manipulated chromosome appeared to be similar to other chromosomes whether the tension was increased or decreased. Further, the myosin II on the detached chromosome dephosphorylated and separated after anaphase onset (Fig 3.6D). These results indicated that the phosphorylation status of myosin II is not sensitive to tension

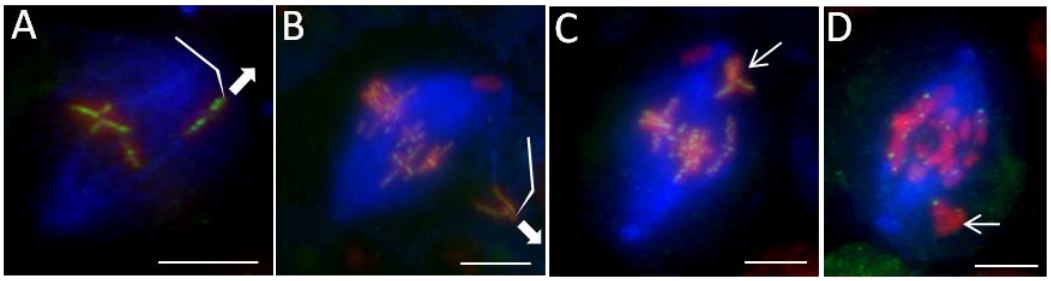

Figure3.6 The phosphorylation status of myosin II on bivalent chromosomes appeared not to be tension-sensitive before anaphase onset.
The tension on chromosome was increased by pulling the chromosome with a microneedle (A and B) or decreased by detaching the chromosome from the spindle (C). The chromosome was pulled by a microneedle vertically (A) or laterally (B). The thick arrows indicate the direction of pulling. The arrow in (C) marks the detached chromosome. The manipulated chromosomes were pulled or detached for 10 minutes. Then fixative was micropipetted around the manipulated cells for fixation. The staining of phosphorylated myosin II showed that the amount of myosin II phosphorylation appeared not to change in response to tension. Myosin II dephosphorylation happened on the detached chromosome (arrow) after anaphase onset. The detached chromosome completely separated (D). Green, phosphorylated myosin II; red, chromosomes; blue, microtubules. n >10. Scale bar, 10 μm

and the dephosphorylation of myosin II is initiated after anaphase onset.

In summary, we have localized phosphorylated myosin II at the interface between the homologous chromosomes in grasshopper spermatocytes. The localization pattern is punctate and dynamic, starting during early prophase and disappearing after the onset of anaphase I. The staining was conspicuously absent from: the univalent sex chromosome; all chromosomes in meiosis II and mitosis; and all chromosomes in drosophila spermatocytes – which commonly lacks homologous recombination. Precocious dephosphorylation of myosin II induced by ml-7 treatment on bivalents caused the disassembly of SMC3 axis between homologous chromosomes in pachytene cells. The ml-7-induced myosin II dephosphorylation also interfered with the maintenance of bivalent structure and condensation of homologous chromosomes in diakinesis cells. Given these results, we believe that phosphorylated myosin II is somehow involved in the pairing and/or crossing over of homologous chromosomes, perhaps by providing the mechanical forces needed for these events. Our reasoning was prompted by the spatial localization pattern of the myosin II in its activated form, and the temporal correlation of its distribution to key locations during meiotic events. The data also suggested that myosin II might mediate the separation of homologous chromosomes before they are able to segregate to the spindle poles. Unlike sister chromatid separation in mitosis (or meiosis II), which is driven primarily by degradation of cohesin, separation of bivalents may require additional breakage at the chiasmata between homologous chromosomes. We reasoned that if phosphorylated myosin II is involved in pairing and/or crossing over of

homologous chromosomes, its dephosphorylation could also be required for separation of homologous chromosomes. In support of this proposition, phosphorylated myosin II localized precisely to the site of homologue separation, and its dephosphorylation coincided with the onset of anaphase I. The bivalent chromosomes could not separate when the dephosphorylation of myosin II was inhibited by Calyculain A.

We hypothesize that the myosin II motor is the long-postulated "bivalent binder" (Nasmyth, 2001) holding homologues together until anaphase onset, and its dephosphorylation is required for separation of the bivalents. We propose that phosphorylated myosin II mediates pairing and/or crossing over between homologous chromosomes during meiosis by providing driving forces via its motor activity to facilitate the recombination process. Following recombination, the motor interacts with chiasmata to hold the homologues together before the onset of anaphase I, then becomes inactivated via perhaps tension-independent dephosphorylation to allow the separation of homologous chromosomes.

Recently, the source of the driving force for rapid chromosome movement (RCM) in mammals has been found: a SUN-KASH complex spans the nuclear envelope, with the SUN protein interacting with telomeres on the inner envelope and KASH interacting with the dynein-dynactin complex on the outer side (Morimoto et al., 2012). In contrast, in budding yeast, RCM is thought to rely on dynamic actin cables (Koszul et al., 2008). However, these mechanisms do not explain the driving force that mediates recombination and separation of homologous bivalents. Thus, our results may help understand both events:

phosphorylated myosin II could mediate homologous recombination by providing mechanical forces, and its dephosphorylation could allow the final separation of homologues at the onset of anaphase I. Nuclear actin and myosins have long been found to play various roles in the nucleus (reviewed in de Lanerolle and Serebryannyy, 2011). For instance, actin is found closely associated with RNA polymerase II and involved in activation of gene transcription (Zhu et al., 2004). Myosin II is involved in cardiac myocyte karyokinesis (Ma et al., 2010). Myosin II in the nucleus is shown to regulate the assembly of the preinitiation complex for transcription of certain genes (Li et al., 2009). Wang et al. have demonstrated that mouse spermatocytes deficient for a specific isoform of myosin II are unable to successfully complete the first meiotic division (Yang et al., 2012). We anticipate that this study will ultimately reveal the driving forces behind homologue pairing and crossing over, and will trigger a reassessment of how homologous chromosomes separate during anaphase I in meiosis. Thus, a new field of research on the role of the myosin II motors in meiosis could be established, and could help provide an understanding of, and eventually treatment for, a subset of medical conditions that arise from meiotic error.

3.3 Method

Micromanipulation, Micropipeting and microscopy

Primary spermatocytes of grasshopper Melanoplus femurrubrum were prepared as described (Alsop and Zhang, 2003). The micromanipulation needle

was made by using a microforge (Narishige, model MF-830)(Zhang, 1999). The micropipeting needle was made by using a Flaming/Brown P-87 micropipette puller (Sutter Instruments)(Chen et al., 2008). Needles were controlled by a micromanipulator (Burleigh MIS-5000 series piezoelectric). Images were recorded with an EM-CCD digital camera (Hamamatsu C9100–12) and processed using Simple PCI (C-image) and Photoshop (Adobe).

Pharmacological manipulation

Myosin II kinase inhibitors, 250 μM ml-7 (Sigma-Aldrich; 50mM in DMSO) and 500 μM VX680 (BioVision; 100 mM in DMSO), were prepared in insect Ringer's buffer. Myosin II phosphatase inhibitor, 5 mM Calyculin A (Cell Signaling Technology), was prepared in insect Ringer's buffer. Inhibitors were micropipetted around target cells, for a 1000+-fold dilution. Cells were treated for 10 minutes, before fixing and immunolabeling.

Immunofluorescence staining

Dividing grasshopper cells were spread on a coverslip, fixed, and stained, as described (Alsop and Zhang, 2004) with minor modifications. Briefly, cells were microfixed (2% glutaraldehyde/2% paraformaldehyde/PBS), then macrofixed (0.1% glutaraldehyde/4% paraformaldehyde/PBS). Phosphorylated myosin II was labeled with rabbit anti-phospho-Myosin Light Chain 2 (Thr18/Ser19) primary antibody (1:100 dilution; Cell Signaling Technology) and Goat anti-Rabbit Alexa-488 (1:300; Molecular Probes/Invitrogen). Microtubules were stained with

sheep anti-alpha/beta tubulin antibody (1:100; Cytoskeleton, Inc.) and Donkey anti-Sheep DyLight 649 (1:300; Jackson ImmunoResearch Laboratories). Non-phosphorylated myosin II was stained by Rabbit anti-myosin light chain antibody (1: 100, Cell Signaling Technology). DNA was stained by 20 ng/ml Hoechst 33342 (Invitrogen) in PBS for 5 minutes. Cells were mounted in Vectashield (Vector Laboratories).

Chapter 4

Conclusion

To maintain genomic integrity of gametes, chromosome segregation and cytokinesis have to be completed precisely. Homologous chromosomes pair and form proper bivalent structure in Prophase I to ensure the normal spindle assembly and homologous chromosome segregation during meiosis I. Cytokinetic proteins are activated and recruited into the region of furrow formation at correct timing to ensure the production of identical daughter cells. Over decades of research, it is still not clear about the physical aspects in the recruitments of cytokinetic proteins during cytokinesis and homologous chromosomes recombination in prophase I. In the first part of my dissertation, I dissected the physical interaction between spindle microtubules and cell cortex during cytokinesis. I showed that dynamic astral microtubules are able to physically move cortical actin filaments into the incipient cleavage furrow. The physical interaction between spindle apparatus and cell cortex is required for the furrow formation. In the second part of my dissertation, I showed the appearance of phosphorylated myosin II on bivalent meiosis I chromosomes. The dynamic distribution of phosphorylated myosin II during meiosis I indicated that phosphorylated myosin II could help meiotic pairing, synapsis and crossing over by providing mechanic force. The dephosphorylation of myosin II is required for separation of homologous chromosomes during anaphase I.

4.1 Dissecting the recruitment of cortical actin filaments into incipient cleavage furrow during cytokinesis

The first part of my dissertation is to dissect how spindle microtubules affect the recruitment of cortical actin filaments during furrow formation. Studies had shown that the physical interaction between spindle apparatus and cell cortex is required for the spatial and temporal control of furrow induction during cytokinesis. Spindle microtubules appear to determine the activation and redistribution of cytokinetic proteins. However, this physical connection had never been directly demonstrated. In this dissertation, I showed the physical connections between astral microtubules and cortical actin network before and during furrow induction by micromanipulating fluorescence-labeled microtubules and actin filaments (Fig 2.1). Astral microtubules physically connected to the pre-existing cortical actin filaments that were flowing toward the region of furrow formation during furrow induction. Physically disrupting this connection blocked the recruitments of actin filaments into the equatorial cortex for the cleavage furrow formation. In CD-treated cells, I showed that dynamic astral microtubules were able to physically move partial dissembled short cortical actin filaments with their positive end tips. On the other hand, disassembly of cortical actin network disconnected cell membrane and spindle microtubules. Demonstrating the existence of the physical interaction between cell cortex and spindle apparatus during cytokinesis explains how spindle apparatus affects the recruitment of cytokinetic proteins. Signals, either positive or negative to furrow formation, can travel on microtubule toward cell cortex

through this physical connection. At the same time, astral microtubules physically move pre-existing actin filaments into cleavage furrow.

4.2 The role of myosin II on meiotic I chromosomes

In the second part of my dissertation, I showed that the phosphorylated myosin II first appeared on synapsed chromosomes in late zygotene and persisted on bivalent chromosomes through the prophase I and metaphase I. After anaphase I onset, myosin II dephosphorylated. Phosphorylated myosin II was found only on bivalent metaphase I chromosomes which undergo crossing over. Phosphorylated myosin II did not appear on non-crossover chromosomes, such as the sex chromosome in Meiosis I, all meiotic II chromosomes and mitotic chromosomes in spermatogonia. I also showed that the dephosphorylation of myosin II induced by ml-7 caused the disassembly of SMC3 axis between homologous chromosomes in pachytene cells and interfered with the maintenance of bivalent structure and condensation of homologous chromosomes in diakinesis cells. Inhibiting the dephosphorylation of myosin II blocked the separation of chromosome after anaphase onset. These results highly suggested that myosin II could provide the mechanic force to hold the pair homologous chromosomes for meiotic chromosome pairing, synapsis and crossing over. The dephosphorylation of myosin II is required for the separation of bivalent chromosomes after anaphase onset. These findings provide a new direction to understand the mechanic aspects of these meiotic-specific events.

Bioliography

Akhmanova, A., & Steinmetz, M. O. (2008). Tracking the ends: a dynamic protein network controls the fate of microtubule tips. Nat Rev Mol Cell Biol, 9(4), 309-322. doi: 10.1038/nrm2369

Albertson, R., Cao, J., Hsieh, T. S., & Sullivan, W. (2008). Vesicles and actin are targeted to the cleavage furrow via furrow microtubules and the central spindle. J Cell Biol, 181(5), 777-790. doi: 10.1083/jcb.200803096

Alsop, G. B., Chen, W., Foss, M., Tseng, K. F., & Zhang, D. (2009). Redistribution of actin during assembly and reassembly of the contractile ring in grasshopper spermatocytes. PLoS One, 4(3), e4892. doi: 10.1371/journal.pone.0004892

Alsop, G. B., & Zhang, D. (2003). Microtubules are the only structural constituent of the spindle apparatus required for induction of cell cleavage. J Cell Biol, 162(3), 383-390. doi: 10.1083/jcb.200301073

Alsop, G. B., & Zhang, D. (2004). Microtubules continuously dictate distribution of actin filaments and positioning of cell cleavage in grasshopper spermatocytes. J Cell Sci, 117(Pt 8), 1591-1602. doi: 10.1242/jcs.01007

Atilgan, E., Burgess, D., & Chang, F. (2012). Localization of cytokinesis factors to the future cell division site by microtubule-dependent transport. Cytoskeleton (Hoboken), 69(11), 973-982. doi: 10.1002/cm.21068

Barr, F. A., & Gruneberg, U. (2007). Cytokinesis: placing and making the final cut. Cell, 131(5), 847-860. doi: 10.1016/j.cell.2007.11.011

Basu, R., & Chang, F. (2007). Shaping the actin cytoskeleton using microtubule tips. Curr Opin Cell Biol, 19(1), 88-94. doi: 10.1016/j.ceb.2006.12.012

Bement, W. M., Benink, H. A., & von Dassow, G. (2005). A microtubule-dependent zone of active RhoA during cleavage plane specification. J Cell Biol, 170(1), 91-101. doi: 10.1083/jcb.200501131

Bhalla, N., & Dernburg, A. F. (2008). Prelude to a division. Annu Rev Cell Dev Biol, 24, 397-424. doi: 10.1146/annurev.cellbio.23.090506.123245

Bonaccorsi, S., Giansanti, M. G., & Gatti, M. (1998). Spindle self-organization and cytokinesis during male meiosis in asterless mutants of Drosophila melanogaster. J Cell Biol, 142(3), 751-761.

Burgoyne, P. S., Mahadevaiah, S. K., & Turner, J. M. (2009). The consequences of asynapsis for mammalian meiosis. Nat Rev Genet, 10(3), 207-216. doi:

10.1038/nrg2505

Cabernard, C., Prehoda, K. E., & Doe, C. Q. (2010). A spindle-independent cleavage furrow positioning pathway. Nature, 467(7311), 91-94. doi: 10.1038/nature09334

Cao, L. G., & Wang, Y. L. (1990). Mechanism of the formation of contractile ring in dividing cultured animal cells. I. Recruitment of preexisting actin filaments into the cleavage furrow. J Cell Biol, 110(4), 1089-1095.

Cao, L. G., & Wang, Y. L. (1996). Signals from the spindle midzone are required for the stimulation of cytokinesis in cultured epithelial cells. Mol Biol Cell, 7(2), 225-232.

Carreno, S., Kouranti, I., Glusman, E. S., Fuller, M. T., Echard, A., & Payre, F. (2008). Moesin and its activating kinase Slik are required for cortical stability and microtubule organization in mitotic cells. J Cell Biol, 180(4), 739-746. doi: 10.1083/jcb.200709161

Chen, W., Foss, M., Tseng, K. F., & Zhang, D. (2008). Redundant mechanisms recruit actin into the contractile ring in silkworm spermatocytes. PLoS Biol, 6(9), e209. doi: 10.1371/journal.pbio.0060209

Chikashige, Y., Haraguchi, T., & Hiraoka, Y. (2007). Another way to move chromosomes. Chromosoma, 116(6), 497-505. doi: 10.1007/s00412-007-0114-8

Chikashige, Y., Tsutsumi, C., Yamane, M., Okamasa, K., Haraguchi, T., & Hiraoka, Y. (2006). Meiotic proteins bqt1 and bqt2 tether telomeres to form the bouquet arrangement of chromosomes. Cell, 125(1), 59-69. doi: 10.1016/j.cell.2006.01.048

D'Avino, P. P. (2009). How to scaffold the contractile ring for a safe cytokinesis - lessons from Anillin-related proteins. J Cell Sci, 122(Pt 8), 1071-1079. doi: 10.1242/jcs.034785

D'Avino, P. P., Savoian, M. S., & Glover, D. M. (2005). Cleavage furrow formation and ingression during animal cytokinesis: a microtubule legacy. J Cell Sci, 118(Pt 8), 1549-1558. doi: 10.1242/jcs.02335

D'Avino, P. P., Takeda, T., Capalbo, L., Zhang, W., Lilley, K. S., Laue, E. D., & Glover, D. M. (2008). Interaction between Anillin and RacGAP50C connects the actomyosin contractile ring with spindle microtubules at the cell division site. J Cell Sci, 121(Pt 8), 1151-1158. doi: 10.1242/jcs.026716

de Lanerolle, P., & Serebryannyy, L. (2011). Nuclear actin and myosins: life without filaments. Nat Cell Biol, 13(11), 1282-1288. doi: 10.1038/ncb2364

de Vries, F. A., de Boer, E., van den Bosch, M., Baarends, W. M., Ooms, M., Yuan, L., . . . Pastink, A. (2005). Mouse Sycp1 functions in synaptonemal complex assembly, meiotic recombination, and XY body formation. Genes Dev, 19(11), 1376-1389. doi: 10.1101/gad.329705

Devore, J. J., Conrad, G. W., & Rappaport, R. (1989). A model for astral stimulation of cytokinesis in animal cells. J Cell Biol, 109(5), 2225-2232.

Ding, D. Q., Haraguchi, T., & Hiraoka, Y. (2010). From meiosis to postmeiotic events: alignment and recognition of homologous chromosomes in meiosis. Febs j, 277(3), 565-570. doi: 10.1111/j.1742-4658.2009.07501.x

Eggert, U. S., Mitchison, T. J., & Field, C. M. (2006). Animal cytokinesis: from parts list to mechanisms. Annu Rev Biochem, 75, 543-566. doi: 10.1146/annurev.biochem.74.082803.133425

Estey, M. P., Kim, M. S., & Trimble, W. S. (2011). Septins. Curr Biol, 21(10), R384-387. doi: 10.1016/j.cub.2011.03.067

Fabian, L., & Forer, A. (2007). Possible roles of actin and myosin during anaphase chromosome movements in locust spermatocytes. Protoplasma, 231(3-4), 201-213. doi: 10.1007/s00709-007-0262-y

Fabian, L., Troscianczuk, J., & Forer, A. (2007). Calyculin A, an enhancer of myosin, speeds up anaphase chromosome movement. Cell Chromosome, 6, 1. doi: 10.1186/1475-9268-6-1

Fehon, R. G., McClatchey, A. I., & Bretscher, A. (2010). Organizing the cell cortex: the role of ERM proteins. Nat Rev Mol Cell Biol, 11(4), 276-287. doi: 10.1038/nrm2866

Field, C. M., & Alberts, B. M. (1995). Anillin, a contractile ring protein that cycles from the nucleus to the cell cortex. J Cell Biol, 131(1), 165-178.

Foe, V. E., Field, C. M., & Odell, G. M. (2000). Microtubules and mitotic cycle phase modulate spatiotemporal distributions of F-actin and myosin II in Drosophila syncytial blastoderm embryos. Development, 127(9), 1767-1787.

Foe, V. E., & von Dassow, G. (2008). Stable and dynamic microtubules coordinately shape the myosin activation zone during cytokinetic furrow formation. J Cell Biol, 183(3), 457-470. doi: 10.1083/jcb.200807128

Fraune, J., Schramm, S., Alsheimer, M., & Benavente, R. (2012). The mammalian synaptonemal complex: protein components, assembly and role in meiotic recombination. Exp Cell Res, 318(12), 1340-1346. doi: 10.1016/j.yexcr.2012.02.018

Fridkin, A., Penkner, A., Jantsch, V., & Gruenbaum, Y. (2009). SUN-domain and KASH-domain proteins during development, meiosis and disease. Cell Mol Life Sci, 66(9), 1518-1533. doi: 10.1007/s00018-008-8713-y

Fujiwara, T., Bandi, M., Nitta, M., Ivanova, E. V., Bronson, R. T., & Pellman, D. (2005). Cytokinesis failure generating tetraploids promotes tumorigenesis in p53-null cells. Nature, 437(7061), 1043-1047. doi: 10.1038/nature04217

Galjart, N. (2010). Plus-end-tracking proteins and their interactions at microtubule ends. Curr Biol, 20(12), R528-537. doi: 10.1016/j.cub.2010.05.022

Gerton, J. L., & Hawley, R. S. (2005). Homologous chromosome interactions in meiosis: diversity amidst conservation. Nat Rev Genet, 6(6), 477-487. doi: 10.1038/nrg1614

Giansanti, M. G., Bonaccorsi, S., Bucciarelli, E., & Gatti, M. (2001). Drosophila male meiosis as a model system for the study of cytokinesis in animal cells. Cell Struct Funct, 26(6), 609-617.

Glover, D. M., Capalbo, L., D'Avino, P. P., Gatt, M. K., Savoian, M. S., & Takeda, T. (2008). Girds 'n' cleeks o' cytokinesis: microtubule sticks and contractile hoops in cell division. Biochem Soc Trans, 36(Pt 3), 400-404. doi: 10.1042/bst0360400

Goldbach, P., Wong, R., Beise, N., Sarpal, R., Trimble, W. S., & Brill, J. A. (2010). Stabilization of the actomyosin ring enables spermatocyte cytokinesis in Drosophila. Mol Biol Cell, 21(9), 1482-1493. doi: 10.1091/mbc.E09-08-0714

Gonsior, S. M., Platz, S., Buchmeier, S., Scheer, U., Jockusch, B. M., & Hinssen, H. (1999). Conformational difference between nuclear and cytoplasmic actin as detected by a monoclonal antibody. J Cell Sci, 112 (Pt 6), 797-809.

Guizetti, J., & Gerlich, D. W. (2010). Cytokinetic abscission in animal cells. Semin Cell Dev Biol, 21(9), 909-916. doi: 10.1016/j.semcdb.2010.08.001

Harper, L., Golubovskaya, I., & Cande, W. Z. (2004). A bouquet of chromosomes. J Cell Sci, 117(Pt 18), 4025-4032. doi: 10.1242/jcs.01363

Hassold, T., & Hunt, P. (2001). To err (meiotically) is human: the genesis of human aneuploidy. Nat Rev Genet, 2(4), 280-291. doi: 10.1038/35066065

Hassold, T., Sherman, S., & Hunt, P. A. (1995). The origin of trisomy in humans. Prog Clin Biol Res, 393, 1-12.

Hiramoto, Y. (1956). Cell division without mitotic apparatus in sea urchin eggs.

Exp Cell Res, 11(3), 630-636.

Hirose, Y., Suzuki, R., Ohba, T., Hinohara, Y., Matsuhara, H., Yoshida, M., . . . Yamamoto, A. (2011). Chiasmata promote monopolar attachment of sister chromatids and their co-segregation toward the proper pole during meiosis I. PLoS Genet, 7(3), e1001329. doi: 10.1371/journal.pgen.1001329

Homolka, D., Jansa, P., & Forejt, J. (2012). Genetically enhanced asynapsis of autosomal chromatin promotes transcriptional dysregulation and meiotic failure. Chromosoma, 121(1), 91-104. doi: 10.1007/s00412-011-0346-5

Hu, C. K., Coughlin, M., Field, C. M., & Mitchison, T. J. (2008). Cell polarization during monopolar cytokinesis. J Cell Biol, 181(2), 195-202. doi: 10.1083/jcb.200711105

Joo, E., Surka, M. C., & Trimble, W. S. (2007). Mammalian SEPT2 is required for scaffolding nonmuscle myosin II and its kinases. Dev Cell, 13(5), 677-690. doi: 10.1016/j.devcel.2007.09.001

Kamijo, K., Ohara, N., Abe, M., Uchimura, T., Hosoya, H., Lee, J. S., & Miki, T. (2006). Dissecting the role of Rho-mediated signaling in contractile ring formation. Mol Biol Cell, 17(1), 43-55. doi: 10.1091/mbc.E05-06-0569

Klein, F., Mahr, P., Galova, M., Buonomo, S. B., Michaelis, C., Nairz, K., & Nasmyth, K. (1999). A central role for cohesins in sister chromatid cohesion, formation of axial elements, and recombination during yeast meiosis. Cell, 98(1), 91-103. doi: 10.1016/s0092-8674(00)80609-1

Koszul, R., Kim, K. P., Prentiss, M., Kleckner, N., & Kameoka, S. (2008). Meiotic chromosomes move by linkage to dynamic actin cables with transduction of force through the nuclear envelope. Cell, 133(7), 1188-1201. doi: 10.1016/j.cell.2008.04.050

Kunda, P., Pelling, A. E., Liu, T., & Baum, B. (2008). Moesin controls cortical rigidity, cell rounding, and spindle morphogenesis during mitosis. Curr Biol, 18(2), 91-101. doi: 10.1016/j.cub.2007.12.051

Kurahashi, H., Kogo, H., Tsutsumi, M., Inagaki, H., & Ohye, T. (2012). Failure of homologous synapsis and sex-specific reproduction problems. Front Genet, 3, 112. doi: 10.3389/fgene.2012.00112

Laporte, D., Zhao, R., & Wu, J. Q. (2010). Mechanisms of contractile-ring assembly in fission yeast and beyond. Semin Cell Dev Biol, 21(9), 892-898. doi: 10.1016/j.semcdb.2010.08.004

Larkin, K., & Danilchik, M. V. (1999). Microtubules are required for completion of cytokinesis in sea urchin eggs. Dev Biol, 214(1), 215-226. doi:

10.1006/dbio.1999.9395

Larkin, K., & Danilchik, M. V. (2001). Three-dimensional Analysis of Laser Scanning Confocal Microscope Sections Reveals an Array of Microtubules in the Cleavage Furrow of Sea Urchin Eggs. Microsc Microanal, 7(3), 265-275. doi: 10.1017.s1431927601010273

Lee, C. Y., Conrad, M. N., & Dresser, M. E. (2012). Meiotic chromosome pairing is promoted by telomere-led chromosome movements independent of bouquet formation. PLoS Genet, 8(5), e1002730. doi: 10.1371/journal.pgen.1002730

Li, Q., & Sarna, S. K. (2009). Nuclear myosin II regulates the assembly of preinitiation complex for ICAM-1 gene transcription. Gastroenterology, 137(3), 1051-1060, 1060.e1051-1053. doi: 10.1053/j.gastro.2009.03.040

Li, X., & Nicklas, R. B. (1997). Tension-sensitive kinetochore phosphorylation and the chromosome distribution checkpoint in praying mantid spermatocytes. J Cell Sci, 110 (Pt 5), 537-545.

Ma, X., Jana, S. S., Conti, M. A., Kawamoto, S., Claycomb, W. C., & Adelstein, R. S. (2010). Ablation of nonmuscle myosin II-B and II-C reveals a role for nonmuscle myosin II in cardiac myocyte karyokinesis. Mol Biol Cell, 21(22), 3952-3962. doi: 10.1091/mbc.E10-04-0293

MacQueen, A. J., Colaiacovo, M. P., McDonald, K., & Villeneuve, A. M. (2002). Synapsis-dependent and -independent mechanisms stabilize homolog pairing during meiotic prophase in C. elegans. Genes Dev, 16(18), 2428-2442. doi: 10.1101/gad.1011602

Maddox, A. S., & Oegema, K. (2003). Deconstructing cytokinesis. Nat Cell Biol, 5(9), 773-776. doi: 10.1038/ncb0903-773b

Matsumura, F. (2005). Regulation of myosin II during cytokinesis in higher eukaryotes. Trends Cell Biol, 15(7), 371-377. doi: 10.1016/j.tcb.2005.05.004

McKee, B. D. (2004). Homologous pairing and chromosome dynamics in meiosis and mitosis. Biochim Biophys Acta, 1677(1-3), 165-180. doi: 10.1016/j.bbaexp.2003.11.017

Morimoto, A., Shibuya, H., Zhu, X., Kim, J., Ishiguro, K., Han, M., & Watanabe, Y. (2012). A conserved KASH domain protein associates with telomeres, SUN1, and dynactin during mammalian meiosis. J Cell Biol, 198(2), 165-172. doi: 10.1083/jcb.201204085

Nasmyth, K. (2001). Disseminating the genome: joining, resolving, and separating

sister chromatids during mitosis and meiosis. Annu Rev Genet, 35, 673-745. doi: 10.1146/annurev.genet.35.102401.091334

Noguchi, T., Arai, R., Motegi, F., Nakano, K., & Mabuchi, I. (2001). Contractile ring formation in Xenopus egg and fission yeast. Cell Struct Funct, 26(6), 545-554.

Odell, G. M., & Foe, V. E. (2008). An agent-based model contrasts opposite effects of dynamic and stable microtubules on cleavage furrow positioning. J Cell Biol, 183(3), 471-483. doi: 10.1083/jcb.200807129

Piekny, A., Werner, M., & Glotzer, M. (2005). Cytokinesis: welcome to the Rho zone. Trends Cell Biol, 15(12), 651-658. doi: 10.1016/j.tcb.2005.10.006

Piekny, A. J., & Maddox, A. S. (2010). The myriad roles of Anillin during cytokinesis. Semin Cell Dev Biol, 21(9), 881-891. doi: 10.1016/j.semcdb.2010.08.002

Pollard, T. D. (2004). Ray Rappaport chronology: Twenty-five years of seminal papers on cytokinesis in the Journal of Experimental Zoology. J Exp Zool A Comp Exp Biol, 301(1), 9-14. doi: 10.1002/jez.a.20000

Qiao, H., Chen, J. K., Reynolds, A., Hoog, C., Paddy, M., & Hunter, N. (2012). Interplay between synaptonemal complex, homologous recombination, and centromeres during mammalian meiosis. PLoS Genet, 8(6), e1002790. doi: 10.1371/journal.pgen.1002790

Rankin, K. E., & Wordeman, L. (2010). Long astral microtubules uncouple mitotic spindles from the cytokinetic furrow. J Cell Biol, 190(1), 35-43. doi: 10.1083/jcb.201004017

Rappaport, R. (1961). Experiments concerning the cleavage stimulus in sand dollar eggs. J Exp Zool, 148, 81-89.

Rappaport, R. (1978). Effects of continual mechanical agitation prior to cleavage in echinoderm eggs. J Exp Zool, 206(1), 1-11. doi: 10.1002/jez.1402060102

Robinson, R. W., & Snyder, J. A. (2005). Localization of myosin II to chromosome arms and spindle fibers in PtK1 cells: a possible role for an actomyosin system in mitosis. Protoplasma, 225(1-2), 113-122. doi: 10.1007/s00709-005-0085-7

Roeder, G. S. (1997). Meiotic chromosomes: it takes two to tango. Genes Dev, 11(20), 2600-2621.

Salmon, E. D. (1989). Cytokinesis in animal cells. Curr Opin Cell Biol, 1(3),

541-547.

Santos, J. L., Cipres, G., & Lacadena, J. R. (1989). A quantitative study of chiasma terminalization in the grasshopper Chorthippus jucundus. Heredity (Edinb), 62 (Pt 1), 51-57.

Sato, A., Isaac, B., Phillips, C. M., Rillo, R., Carlton, P. M., Wynne, D. J., . . . Dernburg, A. F. (2009). Cytoskeletal forces span the nuclear envelope to coordinate meiotic chromosome pairing and synapsis. Cell, 139(5), 907-919. doi: 10.1016/j.cell.2009.10.039

Schmekel, K., Meuwissen, R. L., Dietrich, A. J., Vink, A. C., van Marle, J., van Veen, H., & Heyting, C. (1996). Organization of SCP1 protein molecules within synaptonemal complexes of the rat. Exp Cell Res, 226(1), 20-30. doi: 10.1006/excr.1996.0198

Shen, J. J., Sherman, S. L., & Hassold, T. J. (1998). Centromeric genotyping and direct analysis of nondisjunction in humans: Down syndrome. Chromosoma, 107(3), 166-172.

Shumaker, D. K., Kuczmarski, E. R., & Goldman, R. D. (2003). The nucleoskeleton: lamins and actin are major players in essential nuclear functions. Curr Opin Cell Biol, 15(3), 358-366.

Silverman-Gavrila, R. V., & Forer, A. (2001). Effects of anti-myosin drugs on anaphase chromosome movement and cytokinesis in crane-fly primary spermatocytes. Cell Motil Cytoskeleton, 50(4), 180-197. doi: 10.1002/cm.10006

Silverman-Gavrila, R. V., & Forer, A. (2003). Myosin localization during meiosis I of crane-fly spermatocytes gives indications about its role in division. Cell Motil Cytoskeleton, 55(2), 97-113. doi: 10.1002/cm.10112

Sisson, J. C., Field, C., Ventura, R., Royou, A., & Sullivan, W. (2000). Lava lamp, a novel peripheral golgi protein, is required for Drosophila melanogaster cellularization. J Cell Biol, 151(4), 905-918.

Sonntag Brown, M., Zanders, S., & Alani, E. (2011). Sustained and rapid chromosome movements are critical for chromosome pairing and meiotic progression in budding yeast. Genetics, 188(1), 21-32. doi: 10.1534/genetics.110.125575

Strickland, L. I., Donnelly, E. J., & Burgess, D. R. (2005). Induction of cytokinesis is independent of precisely regulated microtubule dynamics. Mol Biol Cell, 16(10), 4485-4494. doi: 10.1091/mbc.E05-04-0305

Takaesu, N., Jacobs, P. A., Cockwell, A., Blackston, R. D., Freeman, S., Nuccio,

J., . . . Hassold, T. (1990). Nondisjunction of chromosome 21. Am J Med Genet Suppl, 7, 175-181.

Tsai, J. H., & McKee, B. D. (2011). Homologous pairing and the role of pairing centers in meiosis. J Cell Sci, 124(Pt 12), 1955-1963. doi: 10.1242/jcs.006387

Tureci, O., Sahin, U., Zwick, C., Koslowski, M., Seitz, G., & Pfreundschuh, M. (1998). Identification of a meiosis-specific protein as a member of the class of cancer/testis antigens. Proc Natl Acad Sci U S A, 95(9), 5211-5216.

Turner, J. M. (2007). Meiotic sex chromosome inactivation. Development, 134(10), 1823-1831. doi: 10.1242/dev.000018

Valdeolmillos, A. M., Viera, A., Page, J., Prieto, I., Santos, J. L., Parra, M. T., . . . Rufas, J. S. (2007). Sequential loading of cohesin subunits during the first meiotic prophase of grasshoppers. PLoS Genet, 3(2), e28. doi: 10.1371/journal.pgen.0030028

Vazquez, J., Belmont, A. S., & Sedat, J. W. (2002). The dynamics of homologous chromosome pairing during male Drosophila meiosis. Curr Biol, 12(17), 1473-1483.

Viera, A., Santos, J. L., Page, J., Parra, M. T., Calvente, A., Cifuentes, M., . . . Rufas, J. S. (2004). DNA double-strand breaks, recombination and synapsis: the timing of meiosis differs in grasshoppers and flies. EMBO Rep, 5(4), 385-391. doi: 10.1038/sj.embor.7400112

Viera, A., Santos, J. L., & Rufas, J. S. (2009). Relationship between incomplete synapsis and chiasma localization. Chromosoma, 118(3), 377-389. doi: 10.1007/s00412-009-0204-x

White, J. G., & Borisy, G. G. (1983). On the mechanisms of cytokinesis in animal cells. J Theor Biol, 101(2), 289-316.

Wolpert, L. (1960). The mechanics and mechanism of cleavage Int. Rev. Cyt., 10, 163-216.

Woods, L. M., Hodges, C. A., Baart, E., Baker, S. M., Liskay, M., & Hunt, P. A. (1999). Chromosomal influence on meiotic spindle assembly: abnormal meiosis I in female Mlh1 mutant mice. J Cell Biol, 145(7), 1395-1406.

Yamamoto, A., & Hiraoka, Y. (2001). How do meiotic chromosomes meet their homologous partners?: lessons from fission yeast. Bioessays, 23(6), 526-533. doi: 10.1002/bies.1072

Yang, F., Gell, K., van der Heijden, G. W., Eckardt, S., Leu, N. A., Page, D. C., . . .

Wang, P. J. (2008). Meiotic failure in male mice lacking an X-linked factor. Genes Dev, 22(5), 682-691. doi: 10.1101/gad.1613608

Yang, F., & Wang, P. J. (2009). The Mammalian synaptonemal complex: a scaffold and beyond. Genome Dyn, 5, 69-80. doi: 10.1159/000166620

Yang, F., Wei, Q., Adelstein, R. S., & Wang, P. J. (2012). Non-muscle myosin IIB is essential for cytokinesis during male meiotic cell divisions. Dev Biol, 369(2), 356-361. doi: 10.1016/j.ydbio.2012.07.011

Zhang, D., & Nicklas, R. B. (1999). Micromanipulation of chromosomes and spindles in insect spermatocytes. Methods Cell Biol, 61, 209-218.

Zhou, M., & Wang, Y. L. (2008). Distinct pathways for the early recruitment of myosin II and actin to the cytokinetic furrow. Mol Biol Cell, 19(1), 318-326. doi: 10.1091/mbc.E07-08-0783

Zhu, X., Zeng, X., Huang, B., & Hao, S. (2004). Actin is closely associated with RNA polymerase II and involved in activation of gene transcription. Biochem Biophys Res Commun, 321(3), 623-630. doi: 10.1016/j.bbrc.2004.05.229

APPENDIX

Supplemental video legends

Movie 2.1. Cytoskeletal dynamics and the progression of cytokinesis were not obviously affected by the labeling protocols. Movie S1 shows an unmanipulated control cell. Microtubules were labeled by allowing Oregon Green 488 Taxol (paclitaxel) to diffuse into the cell. Actin filaments were labeled by microinjecting Texas Red-X phalloidin into the cell. Movie S1 corresponds to Fig. 2.1A.

Movie 2.2. Interactions between spindle microtubules and cortical actin filaments were revealed by micromanipulation of a cell in mid anaphase (spindle tugged laterally). The physical interaction was probed during mid anaphase by using a microneedle to tug the spindle away from the equatorial cortex, which caused spindle microtubules to drag cortical actin in the direction of movement. Microtubules were labeled by allowing Oregon Green 488 Taxol (paclitaxel) to diffuse into the cell. Actin filaments were labeled by microinjecting Texas Red-X phalloidin into the cell. The arrow in the first frame of the movie indicates the initial position of the microneedle. Movie 2.2 corresponds to Fig. 2.1B.

Movie 2.3. Interactions between spindle microtubules and cortical actin filaments were revealed by micromanipulation of a cell in late anaphase (spindle tugged laterally). The physical interaction was probed during late anaphase by using a

microneedle to tug the spindle away from the equatorial cortex. The membrane was dragged inward when spindle microtubules pulled the cortical actin away from the membrane. Microtubules were labeled by allowing Oregon Green 488 Taxol (paclitaxel) to diffuse into the cell. Actin filaments were labeled by microinjecting Texas Red-X phalloidin into the cell. The arrow in the first frame of the movie indicates the initial position of the microneedle; the arrow in a subsequent frame shows a repositioning of the needle. Movie 2.3 corresponds to Fig. 2.1C.

Movie 2.4. Interactions between spindle microtubules and cortical actin filaments were revealed by micromanipulation of a cell in late anaphase (spindle tugged poleward). The physical interaction between spindle microtubules and cortical actin filaments was probed during late anaphase by using a microneedle to tug the spindle away from the polar cortex. Note the membrane indentation at the lower pole, as the spindle is pulled upwards. Microtubules were labeled by allowing Oregon Green 488 Taxol (paclitaxel) to diffuse into the cell. Actin filaments were labeled by microinjecting Texas Red-X phalloidin into the cell. The arrow in the first frame of the movie indicates the initial position of the microneedle. Movie 2.4 corresponds to Fig. 2.1D.

Movie 2.5. Microtubule interaction with flowing cortical actin filaments, as seen by manipulation of an aster in a monopolar spindle. The physical interaction was probed during the induced flow of cortical actin. (Flow had been induced when a collapsed bipolar spindle self-assembled into a monopolar spindle.) Microtubules

were labeled by allowing Oregon Green 488 Taxol (paclitaxel) to diffuse into the cell. Actin filaments were labeled by microinjecting Texas Red-X phalloidin into the cell. The arrow in the first frame of the movie indicates the initial position of the microneedle. Movie 2.5 corresponds to Fig. 2.2.

Movie 2.6. Formation of the cleavage furrow required interaction between microtubules and actin filaments. Furrow formation could be locally disrupted by physically disconnecting the microtubules from the cell cortex. (The red spot on the right side of the cell is an actin-containing scar from a previous cell division.) Microtubules were labeled by allowing Oregon Green 488 Taxol (paclitaxel) to diffuse into the cell. Actin filaments were labeled by microinjecting Texas Red-X phalloidin into the cell. Movie 2.6 corresponds to Fig. 2.3A.

Movie 2.7. Formation of the cleavage furrow required interaction between microtubules and actin filaments (rotation). The three-dimensional distribution of actin confirmed the topology of a partially formed cleavage furrow. The cell's furrow was disrupted by micromanipulation of the spindle. Movie 2.7 corresponds to Fig. 2.3B.

Movie 2.8. Waving microtubules moved Cytochalasin D-induced cortical actin aggregates. An elongating microtubule was able to push a cortical actin aggregate. Microtubules were labeled by allowing Oregon Green 488 Taxol (paclitaxel) to

diffuse into the cell. Actin filaments were labeled by microinjecting Texas Red-X phalloidin into the cell. Movie 2.8 corresponds to Fig. 2.4A.

Movie 2.9. Waving microtubules moved Cytochalasin D-induced cortical actin aggregates (ROI). Microtubules were labeled by allowing Oregon Green 488 Taxol (paclitaxel) to diffuse into the cell. Actin filaments were labeled by microinjecting Texas Red-X phalloidin into the cell. Movie 2.9 is a selected area of Movie 2.8 (Fig. 2.4B is a portion of this movie).

Movie 2.10. Waving microtubules, seen at low density, moved Cytochalasin D-induced cortical actin aggregates. In a cell with an asymmetrically localized spindle, microtubules contacting the cortex distal to the spindle were less densely packed, making it easier to observe their interactions as they moved the cortical actin aggregates. Microtubules were labeled by allowing Oregon Green 488 Taxol (paclitaxel) to diffuse into the cell. Actin filaments were labeled by microinjecting Texas Red-X phalloidin into the cell. Movie 2.10 corresponds to Fig. 2.4C.

Movie 2.11 Microtubule dynamics appeared unaffected by CD treatment. Dynamic astral microtubules were still able to elongate and wave in CD-treated cells. Astral microtubules from the two spindle halves pivoted towards the equator where they made contact and appeared to interdigitate with microtubules from the opposing aster, forming stable microtubules at the furrow region. Microtubules were labeled by allowing Oregon Green 488 Taxol (paclitaxel) to diffuse into the cell.

Movie 2.12 The connection between membrane and microtubule was mediated by the actin network. The physical interaction between spindle microtubules and cortical actin filaments or the membrane was tested in the presence of CD. Microtubules were labeled by allowing Oregon Green 488 Taxol (paclitaxel) to diffuse into the cell. Actin filaments were labeled by microinjecting Texas Red-X phalloidin into the cell. The arrow in the first frame of the movie indicates the initial position of the microneedle. Movie 2.12 corresponds to Fig. 2.5.

Movie 3.1 The Dephosphorylation of Myosin II induced by ml-7 caused the misalignment of metaphase I chromosomes.

Movie 3.2 The detached chromosomes in a metaphase cell cannot move back to the equator plate in the presence of ml-7.

Movie3.3 In normal condition, the detached chromosome can move back to equator plate soon.